reviews

molecular pharmaceutics

Interplay of Transporters and Enzymes in Drug and Metabolite Processing

K. Sandy Pang,* Han-Joo Maeng, and Jianghong Fan

Leslie L. Dan Faculty of Pharmacy, University of Toronto, Toronto, Ontario, Canada M5S 3M2

Received October 14, 2009; Revised Manuscript Received November 4, 2009; Accepted November 5, 2009

Abstract: This review highlights the "interplay" between enzymes and transporters, essential components of eliminating organs for drug removal. The understanding of the interplay is important in terms of deciphering the change of one eliminatory pathway on compensatory mechanisms in drug disposal, and, ultimately, their importance in drug−drug interactions. Controversy existed on the explanation underlying the interplay between transporters and enzymes in the Caco-2 cell monolayer or cell culture systems, but less so on eliminating organs such as the intestine and liver. For the Caco-2 system, the increase in the mean residence time (MRT) accompanying increased secretion had been construed as the basis for increased metabolism. We hold the opposite view and assert that increased secretion should evoke a decrease in metabolism due to the competition between the enzyme and apical efflux transporter for the drug within the cell. To illustrate this point, simulations on the MRT, fraction of dose metabolized (f_{met}) and the extraction ratio (ER) as defined by various investigators under linear and nonlinear metabolic conditions were compared to observed data and the trends upon induction/inhibition of secretion. The conclusion is that the f_{met} is the more appropriate index to reflect the extent of metabolism in transporter−enzyme interplay, since the parameter captures drug metabolism in the cell when its contents in the apical, cell, and basolateral compartments or the entire dose is considered to be available for metabolism. This parameter for metabolism (f_{met}) bears a reciprocal relationship to the secretory intrinsic clearance and is in concordance with the notion that both the enzyme and apical transporter compete for the cellular substrate within. For the liver and intestine, several physiologically based pharmacokinetic (PBPK) models that contain transporters and enzymes were utilized, together with the solved equations for the area under the curve (AUC), metabolic, excretory, and total clearance (CL) to shed meaningful insight of how the inhibition of one pathway can result in a higher AUC and therefore a reduced total clearance for drug, but a higher apparent clearance of the alternate pathway; induction of the same pathway would lead to an increased total clearance but decreased drug AUC, and reduced clearance of the alternate pathway. The use of an increased MRT to explain increased extents of metabolism upon increased apical excretion is not tenable in these organs or "open systems" since the MRT of drug in the cell is reduced with irreversible loss from biliary excretion or hastened gastrointestinal transit of the secreted drug in the lumen. Data in the literature for the Caco-2 system, knockout animals and organ perfusion systems were discussed in relation to these concepts on clearance based on fundamental, pharmacokinetic theory. The shortcomings in data interpretation were discussed. The general conclusion is that a reciprocal relationship exists between the clearances related to enzymes and apical transporters due to their competition for the substrate within the cell, and is a relationship independent of the MRT of drug in the system.

Keywords: Transporter; enzyme; interplay; metabolism; excretion; Caco-2; physiologically based pharmacokinetic (PBPK) model; liver; intestine; area under the curve (AUC); clearance (CL)

I. Introduction

Drug elimination is a complex process that is governed by drug influx into an organ, followed by efflux back to the circulation, cellular metabolism and excretion. Basolateral influx and efflux transporters modulate the extent of elimination by regulating drug accumulation in the cell. Cellular binding proteins further modulate the "free" form, the unbound drug species that enters the cell and undergoes elimination.[1−4] The net outcome depends on the interaction between the drug and proteins for binding, transport and metabolism, and is reliant on the intricate and dynamic

* Corresponding author. Mailing address: Leslie Dan Faculty of Pharmacy, University of Toronto, 144 College Street, Toronto, Ontario, Canada M5S 3M2. E-mail: ks.pang@utoronto.ca. Phone: 416-978-6164. Fax: 416-978-8511.

10.1021/mp900258z
Published on Web 11/05/2009

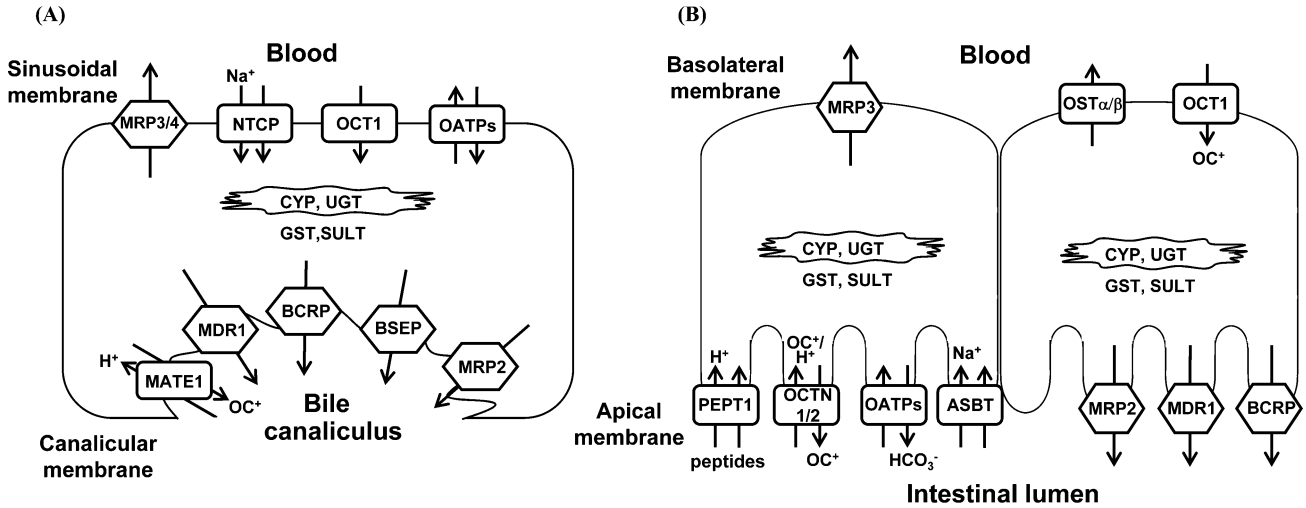

Figure 1. The coexistence of transporters and enzymes in eliminating organs: (A) the liver and (B) the intestine.

processes that control the unbound substrate concentration within the cell. Basolateral influx and efflux transporters regulate the extent of drug accumulation intracellularly, and enzymes and excretory transporters modulate the cellular concentration via metabolism and excretion, respectively. Excretion is usually irreversible when the content is lost permanently unless there is some mechanism for reabsorption of either the parent compound or the metabolite that can refurnish the parent drug. The occurrence depends very much on the organ under consideration. Both the intestine and kidneys are capable of reabsorbing the drug and metabolite at the apical membranes.

The amounts of enzymes differ among organs, with the liver being endowed with the most abundance of enzymes among the organs. Biotransformation by phase I pathways confers functional groups to byproducts that are susceptible to phase II metabolism. Phase I metabolism occurs predominantly with the cytochrome P450 enzymes, whereas phase II metabolism occurs as conjugation reactions that include the UDP-glucuronosyltransferases (UGTs), sulfotransferases (SULTs), glutathione S-transferases (GSTs), methyltransferases, N-acetyltransferases, and amino acid N-acetyltransferase.

The transporters are also organ-specific and display a wide but varying distribution in the body (Figure 1).[5−7] Transporters may be broadly categorized into the solute carrier family members (*SLC*) that mediate the influx or bidirectional movement of drugs across the cell membrane and the ATP-binding cassette (*ABC*) family that effects excretion (Figure 1). The *SLC* transporters include the organic anion transporting polypeptide (*SLCO*) subfamily consisting of organic anion transporting polypeptides (OATPs/*SLC21*) that are involved in the cellular uptake of a broad variety of substrates. Examples are the oligopeptide transporters (*SLC15*) that operate as H^+-coupled symporters and transport di- and tripeptides or peptidomimetics and the organic anion/cation/zwitterion transporter (*SLC22*) family that transports organic anions and cations. Recently, the multidrug and toxin extrusion family (MATE/*SLC47*) has been identified as the H^+/organic cation antiporter present mostly in the kidney as an efflux transporter that is energized by an inwardly directed proton gradient to overcome the outside positive membrane potential.[8] Two sodium-dependent transporters, the apical sodium-dependent bile acid transporter (ASBT/*SLC10A2*), a selective bile acid transporter that reclaims the excreted bile acids in the intestine, and the sodium-dependent cotransporting polypeptide (NTCP/*SLC10A1*) that facilitates the uptake of bile acids into the liver, are partially responsible for the homeostasis of bile acids in the body.[9]

The excretion of drugs and metabolites into the intestinal lumen or bile is mediated by ABC transporters: the P-

(1) Liu, L.; Pang, K. S. The Roles of Transporters and Enzymes in Hepatic Drug Processing. *Drug Metab. Dispos.* **2005**, *33*, 1–9.
(2) Liu, S.; Tam, D.; Chen, X.; Pang, K. S. P-Glycoprotein and an Unstirred Water Layer Barring Digoxin Absorption in the Vascularly Perfused Rat Small Intestine Preparation: Induction Studies with Pregnenolone-16alpha-Carbonitrile. *Drug Metab. Dispos.* **2006**, *34*, 1468–1479.
(3) Pang, K. S.; Weiss, M.; Macheras, P. Advanced Pharmacokinetic Models Based on Organ Clearance, Circulatory, and Fractal Concepts. *AAPS J.* **2007**, *9*, E268–283.
(4) Pang, K. S.; Morris, M. E.; Sun, H. Formed and Preformed Metabolites: Facts and Comparisons. *J. Pharm. Pharmacol.* **2008**, *60*, 1247–1275.
(5) Eloranta, J. J.; Kullak-Ublick, G. A. Coordinate Transcriptional Regulation of Bile Acid Homeostasis and Drug Metabolism. *Arch. Biochem. Biophys.* **2005**, *433*, 397–412.
(6) Shitara, Y.; Horie, T.; Sugiyama, Y. Transporters as a Determinant of Drug Clearance and Tissue Distribution. *Eur. J. Pharm. Sci.* **2006**, *27*, 425–446.
(7) Russel, F. G.; Koenderink, J. B.; Masereeuw, R. Multidrug Resistance Protein 4 (Mrp4/Abcc4): A Versatile Efflux Transporter for Drugs and Signalling Molecules. *Trends Pharmacol. Sci.* **2008**, *29*, 200–207.
(8) Moriyama, Y.; Hiasa, M.; Matsumoto, T.; Omote, H. Multidrug and Toxic Compound Extrusion (MATE)-Type Proteins as Anchor Transporters for the Excretion of Metabolic Waste Products and Xenobiotics. *Xenobiotica* **2008**, *38*, 1107–1118.
(9) Trauner, M.; Boyer, J. L. Bile Salt Transporters: Molecular Characterization, Function, and Regulation. *Physiol. Rev.* **2003**, *83*, 633–671.

glycoprotein (P-gp or MDR1/*ABCB1*) and breast cancer resistance protein (BCRP/*ABCG2*). Others members are the multidrug resistance associated protein *ABCC* subfamily, MRP2/*ABCC2*, MRP3/*ABCC3,* and MRP4/*ABCC4*.[5,6,10,11] MRP2 is located at the apical membrane of polarized cells, and is responsible for the excretion of anionic drugs and conjugates.[12] MRP3 mediates the cellular efflux of some drug conjugates,[13] whereas MRP4, localized at the basolateral membrane of the liver and the apical membrane of renal proximal tubule cells,[14,15] exhibits a higher apical abundance and mediates apical and basolateral efflux of the intestine.[7,16] Mrp3 functions as an alternative route for the export of bile acids and glucuronides from cholestatic hepatocytes.[17] In the liver, the bile salt export pump (BSEP/*ABCB11*) is unique and selective for the canalicular excretion transport of bile acids.[18]

II. Experimental Systems and Controversy

An understanding of the "interplay" between transporters and enzymes is important in terms of deciphering the changes in clearance upon alteration of one pathway and what effect this imposes on compensatory mechanisms in drug−drug interactions (DDIs).[19−21] Much investigation on this topic has focused on organ perfusion systems and the Caco-2 monolayer, systems in which both transporters and enzymes are present. The advantages of these systems are that pathways are readily perturbed with use of inhibitors or inducers, and that individual events are confined to the organ/tissue of interest. Gene knockout animals are routinely used for examination of substrates in absence of that gene. Of note is the *mdr1a/1b*(−/−) or P-gp knockout mice[22] and the TR$^-$ or EHBR rat[23−25] that lacks the Mrp2 gene. In addition to the *mdr1* gene KO model or mutant animals, *in vitro* cell lines that overexpress P-gp or enzymes and animal and clinical trials using P450 and P-gp modulators have allowed for the comparison of data *in vitro* and *in vivo* and species-related difference in P-gp and enzyme activities and their interplay.[26] However, some inhibitors may act as dual inhibitors of both transporters and enzymes, or exert inhibition/induction at varying doses, or may not be specific enough to inhibit the enzyme or transporter consistently.[27] Examples in the literature pertaining to transporter−enzyme interplay are numerous. However, confusing and opposite views exist on the evaluation of the effect of enzymes on alternate, competing metabolic or excretory pathways. Likewise, similar controversies exist in elimination organs such as the intestine and liver.

In this review, we will examine concepts pertaining to the transporter−enzyme interplay. Basic pharmacokinetic models

(10) van Montfoort, J. E.; Hagenbuch, B.; Groothuis, G. M.; Koepsell, H.; Meier, P. J.; Meijer, D. K. Drug Uptake Systems in Liver and Kidney. *Curr. Drug Metab.* **2003**, *4*, 185–211.

(11) Robey, R. W.; Polgar, O.; Deeken, J.; To, K. W.; Bates, S. E. Abcg2: Determining Its Relevance in Clinical Drug Resistance. *Cancer Metastasis Rev.* **2007**, *26*, 39–57.

(12) Nies, A. T.; Schwab, M.; Keppler, D. Interplay of Conjugating Enzymes with Oatp Uptake Transporters and Abcc/Mrp Efflux Pumps in the Elimination of Drugs. *Expert Opin. Drug Metab. Toxicol.* **2008**, *4*, 545–568.

(13) Borst, P.; de Wolf, C.; van de Wetering, K. Multidrug Resistance-Associated Proteins 3, 4, and 5. *Pfluegers Arch.* **2007**, *453*, 661–673.

(14) Rius, M.; Nies, A. T.; Hummel-Eisenbeiss, J.; Jedlitschky, G.; Keppler, D. Cotransport of Reduced Glutathione with Bile Salts by Mrp4 (Abcc4) Localized to the Basolateral Hepatocyte Membrane. *Hepatology* **2003**, *38*, 374–384.

(15) van Aubel, R. A.; Smeets, P. H.; Peters, J. G.; Bindels, R. J.; Russel, F. G. The Mrp4/Abcc4 Gene Encodes a Novel Apical Organic Anion Transporter in Human Kidney Proximal Tubules: Putative Efflux Pump for Urinary cAMP and cGMP. *J. Am. Soc. Nephrol.* **2002**, *13*, 595–603.

(16) Li, C.; Krishnamurthy, P. C.; Penmatsa, H.; Marrs, K. L.; Wang, X. Q.; Zaccolo, M.; Jalink, K.; Li, M.; Nelson, D. J.; Schuetz, J. D.; Naren, A. P. Spatiotemporal Coupling of cAMP Transporter to CFTR Chloride Channel Function in the Gut Epithelia. *Cell* **2007**, *131*, 940–951.

(17) Belinsky, M. G.; Dawson, P. A.; Shchaveleva, I.; Bain, L. J.; Wang, R.; Ling, V.; Chen, Z. S.; Grinberg, A.; Westphal, H.; Klein-Szanto, A.; Lerro, A.; Kruh, G. D. Analysis of the in Vivo Functions of Mrp3. *Mol. Pharmacol.* **2005**, *68*, 160–168.

(18) Stieger, B.; Meier, Y.; Meier, P. J. The Bile Salt Export Pump. *Pfluegers Arch.* **2007**, *453*, 611–620.

(19) Wacher, V. J.; Silverman, J. A.; Zhang, Y.; Benet, L. Z. Role of P-Glycoprotein and Cytochrome P450 3A in Limiting Oral Absorption of Peptides and Peptidomimetics. *J. Pharm. Sci.* **1998**, *87*, 1322–1330.

(20) Schuetz, E. G.; Schinkel, A. H. Drug Disposition as Determined by the Interplay between Drug-Transporting and Drug-Metabolizing Systems. *J. Biochem. Mol. Toxicol.* **1999**, *13*, 219–222.

(21) Tachibana, T.; Kato, M.; Watanabe, T.; Mitsui, T.; Sugiyama, Y. Method for Predicting the Risk of Drug-Drug Interactions Involving Inhibition of Intestinal Cyp3A4 and P-Glycoprotein. *Xenobiotica* **2009**, *39*, 430–443.

(22) Schinkel, A. H.; Mayer, U.; Wagenaar, E.; Mol, C. A.; van Deemter, L.; Smit, J. J.; van der Valk, M. A.; Voordouw, A. C.; Spits, H.; van Tellingen, O.; Zijlmans, J. M.; Fibbe, W. E.; Borst, P. Normal Viability and Altered Pharmacokinetics in Mice Lacking Mdr1-Type (Drug-Transporting) P-Glycoproteins. *Proc. Natl. Acad. Sci. U.S.A.* **1997**, *94*, 4028–4033.

(23) Jansen, P. L.; Peters, W. H.; Meijer, D. K. Hepatobiliary Excretion of Organic Anions in Double-Mutant Rats with a Combination of Defective Canalicular Transport and Uridine 5′-Diphosphate-Glucuronyltransferase Deficiency. *Gastroenterology* **1987**, *93*, 1094–1103.

(24) Yamazaki, K.; Mikami, T.; Hosokawa, S.; Tagaya, O.; Nozaki, Y.; Kawaguchi, A.; Funami, H.; Katoh, H.; Yamamoto, N.; Wakabayashi, T. A New Mutant Rat with Hyperbilirubinuria (Hyb). *J. Hered.* **1995**, *86*, 314–317.

(25) Ito, K.; Suzuki, H.; Hirohashi, T.; Kume, K.; Shimizu, T.; Sugiyama, Y. Molecular Cloning of Canalicular Multispecific Organic Anion Transporter Defective in EHBR. *Am. J. Physiol.* **1997**, *272*, G16–22.

(26) Chen, C.; Liu, X.; Smith, B. J. Utility of Mdr1-Gene Deficient Mice in Assessing the Impact of P-Glycoprotein on Pharmacokinetics and Pharmacodynamics in Drug Discovery and Development. *Curr. Drug Metab.* **2003**, *4*, 272–291.

(27) Kim, R. B.; Wandel, C.; Leake, B.; Cvetkovic, M.; Fromm, M. F.; Dempsey, P. J.; Roden, M. M.; Belas, F.; Chaudhary, A. K.; Roden, D. M.; Wood, A. J.; Wilkinson, G. R. Interrelationship between Substrates and Inhibitors of Human Cyp3A and P-Glycoprotein. *Pharm. Res.* **1999**, *16*, 408–414.

and theory will be used to illustrate how these events play out. A catenary model for the Caco-2 system and physiologically based pharmacokinetic (PBPK) models for the liver and intestine that include consideration of influx/efflux transporters and enzymes and excretory transporters will be used to illustrate the interplay between transporters and enzymes. Analytical solutions based on PBPK models have been successfully solved and will be used to illustrate the influence of these variables on the area under the concentration−time curve (AUC) of the parent drug and its metabolites and therefore the clearances (CL). The developed concepts, based on the fundamentals of rate equations on mass transfer, should be insightful and alleviate further confusion. The knowledge gained would further explain the mechanisms of drug−drug interactions.

III. Modeling and Simulations

Pharmacokinetic models are useful tools in the understanding of transporter−enzyme interplay. The activities of the enzyme or transporter may be expressed as the intrinsic clearance or CL_{int}, which, under first-order conditions, equals the ratio, V_{max}/K_m, or maximum velocity/Michaelis−Menten constant, and is the volume of cellular water that is cleared of the drug per unit time.[28,29] In the absence of a membrane barrier for drug entry, multiplication of the metabolic intrinsic clearance, $CL_{int,met}$, to the (unbound) substrate concentration [S] provides the overall reaction rate.

The Caco-2 system may be modeled as a catenary model to describe transport and metabolic processes arising from the compartments where CL_{d1} and CL_{d2}, CL_{d3} and CL_{d4} are the passive diffusion clearances for influx and efflux at the basolateral and apical membranes, respectively, for the drug. CL_{in} and CL_{ef} are the transporter-mediated influx and efflux intrinsic clearances on the basolateral membrane (Figure 2). However, for intact organs such as the liver, intestine, and kidney, physiologically based pharmacokinetic (PBPK) models are used (see Figures 5, 8, and 9 to follow) with additional parameters such as the blood flow to the organ and membrane barriers as additional determinants. Usually, a well-mixed compartment is considered for the organ; this suggests that enzyme or substrate gradients within the compartment are irrelevant. Each compartment of discrete volume that represents an organ/tissue is perfused by blood flow, and the organs or tissues are interconnected by the circulation. The total transmembrane activity at the basolateral membrane [denoted as the transport clearance for influx (CL_{in}) or efflux (CL_{ef})] consists of summed entities of the passive diffusion clearance (CL_{diff}) and the transporter-mediated clearance ($CL_{transporter}$). Several PBPK models that include consideration of influx/efflux transporters and enzymes have been utilized to describe liver, intestine, and renal clearances.[4] The usefulness of the model is that solutions that relate blood flow, protein binding, transporters, and enzymes are derived by matrix inversion from the rate equations for drug and metabolite.[4,30,31] The solutions would highlight the influence of transporters and enzymes on the various parameters: efflux ratio (EfR), AUC and CL determinations. These concepts will be covered in the ensuing sections.

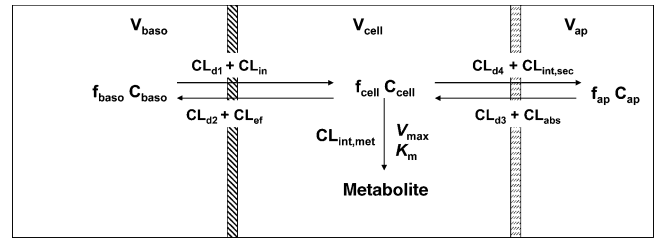

Figure 2. Schematic presentation of the Caco-2 cell monolayer in a catenary model that is composed of the basolateral (baso), cell, and apical (ap) compartments. V, f, and C denote the volume, unbound fraction, and the concentration of drug, respectively; Metabolite denotes the total amount of the formed metabolite; CL_{d1} and CL_{d2}, CL_{d3} and CL_{d4} are the passive diffusion clearances for influx and efflux at the basolateral and apical membranes, respectively, for the drug. CL_{in} and CL_{ef} are the transporter-mediated influx and efflux intrinsic clearances on the basolateral membrane; CL_{abs} and $CL_{int,sec}$ denote transporter-mediated intrinsic clearances of absorption and efflux on the apical membrane, respectively; $CL_{int,met}$ is the metabolic intrinsic clearance. Under nonlinear conditions, CL_{in}, CL_{ef}, CL_{abs}, $CL_{int,sec}$ and $CL_{int,met}$ are replaced by the $V_{max}/(K_m + C_u)$ under nonlinear conditions, where C_u, is the unbound drug concentration (modified from Sun et al.[31] with permission).

IV. Transporter−Enzyme Interplay in the Caco-2 Cell System

The Caco-2 cell monolayer is a closed system in which blood flow is absent. The Caco-2 cell monolayer has been used widely for high throughput screening of drug permeability and identification of substrates, inhibitors, and inducers of intestinal transporters, especially with respect to the P-gp. The equation used to categorize the permeability coefficient (P_{app}) of substrates is given by

$$P_{app} = \frac{\Delta A_R/\Delta t}{\text{area} \times 60 \times C_{D,0}} \quad (1)$$

where ΔA_R is the difference in amount at the receiver side (R) for the given time interval (Δt), and $\Delta A_R/\Delta t$ is the rate of change of drug amount in the receiver side or the (linear)

(28) Gillette, J. R. Factors Affecting Drug Metabolism. *Ann. N.Y. Acad. Sci.* **1971**, *179*, 43–66.

(29) Wilkinson, G. R.; Shand, D. G. Commentary: A Physiological Approach to Hepatic Drug Clearance. *Clin. Pharmacol. Ther.* **1975**, *18*, 377–390.

(30) Sirianni, G. L.; Pang, K. S. Organ Clearance Concepts: New Perspectives on Old Principles. *J. Pharmacokinet. Biopharm.* **1997**, *25*, 449–470.

(31) Sun, H.; Pang, K. S. Disparity in Intestine Disposition between Formed and Preformed Metabolites and Implications: A Theoretical Study. *Drug Metab. Dispos.* **2009**, *37*, 187–202.

slope of the cumulative amount of drug appearing in the receiver side versus time plot; area is the cross sectional area of the cell monolayer; $C_{D,0}$ is the initial or loading concentration given into the donor compartment at time = 0, and 60 is the conversion factor of minute to second. Equation 1 is derived from Fick's law that describes the permeation of solutes across a single membrane by passive diffusion only. Several assumptions need to be made for an accurate estimate of permeability. First, the amount of drug transported through the monolayer must be proportional to time. Second, the system has to comply with "sink conditions", implying that drug molecules reaching the receiver side will not return to the cell monolayer or donor compartment. Practically speaking, if the concentration in the receiver side is less than 10% of the drug concentration in the donor side, "sink conditions" are considered to prevail. Lastly, cellular accumulation and nonspecific binding to the apparatus that may result in underestimation of the P_{app} are absent.[32]

Accordingly, EfR, or $P_{app(B\rightarrow A)}/P_{app(A\rightarrow B)}$, the ratio of the apparent permeability in the B → A to that in the A → B direction, is used to define transporter-assisted efflux by apical transporters such as the P-gp. An EfR value that exceeds 1.5 suggests the possibility that the test compound is a substrate of an apical efflux transporter. It was further shown in this system that, upon treatment with 1α,25-dihydroxyvitamin D_3 or transfection with CYP3A4 cDNA, levels of CYP3A4 would be increased.[33,34] Since the Caco-2 system contains both CYP3A4 and P-gp, much literature exists to define the interplay between P-gp and CYP3A4.

It has been proposed that extension of cellular transit time (mean residence time or MRT) is the underlying mechanism whereby the apical efflux activity of P-gp can influence metabolism.[35] A considerable amount of work adheres to the conclusion that an increase in P-gp (or apical excretion) activity would result in increased metabolism by increasing the MRT.[36−43] An opposite view, however, is held by our laboratory and others who suggest that an increase in P-gp activity should decrease the rate of metabolism despite the increase in MRT.[32,44,45] The more important parameter to consider is the concentration within the cell, which, upon integration, is the area under the curve or the exposure. The concentration or the exposure, when multiplied to the intrinsic clearance for metabolism, furnishes the rate of metabolism and the dose, respectively. A reciprocal relationship should hold since the pathways compete for the substrate, thus a higher activity of one pathway should reduce the apparent rate from other pathways.

The controversy had stemmed from the use of different parameters to normalize the extent of metabolite formation. The early work of Hochman used the following equation to express the extent of metabolism in cell transport studies as the ratio of the summed total amount of metabolite formed (∑metabolites) and the amount of drug in the receiver compartment ($P_{receiver}$):[37]

$$\text{metabolite/parent ratio} = \frac{\sum \text{metabolites}}{P_{\text{receiver}}} \qquad (2)$$

Fisher and colleagues then defined the estimate of metabolite formation as the extraction ratio (ER), and added the summed metabolite amount in the denominator of eq 2.[36]

(32) Sun, H.; Pang, K. S. Permeability, Transport, and Metabolism of Solutes in Caco-2 Cell Monolayers: A Theoretical Study. *Drug Metab. Dispos.* **2008**, *36*, 102–123.

(33) Cummins, C. L.; Mangravite, L. M.; Benet, L. Z. Characterizing the Expression of Cyp3A4 and Efflux Transporters (P-gp, Mrp1, and Mrp2) in Cyp3A4-Transfected Caco-2 Cells after Induction with Sodium Butyrate and the Phorbol Ester 12-O-Tetradecanoylphorbol-13-Acetate. *Pharm. Res.* **2001**, *18*, 1102–1109.

(34) Schmiedlin-Ren, P.; Thummel, K. E.; Fisher, J. M.; Paine, M. F.; Watkins, P. B. Induction of Cyp3A4 by 1 α,25-Dihydroxyvitamin D_3 Is Human Cell Line-Specific and Is Unlikely to Involve Pregnane X Receptor. *Drug Metab. Dispos.* **2001**, *29*, 1446–1453.

(35) Gan, L. S.; Moseley, M. A.; Khosla, B.; Augustijns, P. F.; Bradshaw, T. P.; Hendren, R. W.; Thakker, D. R. Cyp3A-Like Cytochrome P450-Mediated Metabolism and Polarized Efflux of Cyclosporin A in Caco-2 Cells. *Drug Metab. Dispos.* **1996**, *24*, 344–349.

(36) Fisher, J. M.; Wrighton, S. A.; Watkins, P. B.; Schmiedlin-Ren, P.; Calamia, J. C.; Shen, D. D.; Kunze, K. L.; Thummel, K. E. First-Pass Midazolam Metabolism Catalyzed by 1α,25-Dihydroxy Vitamin D_3-Modified Caco-2 Cell Monolayers. *J. Pharmacol. Exp. Ther.* **1999**, *289*, 1134–1142.

(37) Hochman, J. H.; Chiba, M.; Nishime, J.; Yamazaki, M.; Lin, J. H. Influence of P-Glycoprotein on the Transport and Metabolism of Indinavir in Caco-2 Cells Expressing Cytochrome P-450 3A4. *J. Pharmacol. Exp. Ther.* **2000**, *292*, 310–318.

(38) Cummins, C. L.; Jacobsen, W.; Benet, L. Z. Unmasking the Dynamic Interplay between Intestinal P-Glycoprotein and Cyp3A4. *J. Pharmacol. Exp. Ther.* **2002**, *300*, 1036–1045.

(39) Cummins, C. L.; Jacobsen, W.; Christians, U.; Benet, L. Z. Cyp3A4-Transfected Caco-2 Cells as a Tool for Understanding Biochemical Absorption Barriers: Studies with Sirolimus and Midazolam. *J. Pharmacol. Exp. Ther.* **2004**, *308*, 143–155.

(40) Benet, L. Z.; Cummins, C. L.; Wu, C. Y. Unmasking the Dynamic Interplay between Efflux Transporters and Metabolic Enzymes. *Int. J. Pharm.* **2004**, *277*, 3–9.

(41) Chan, L. M.; Cooper, A. E.; Dudley, A. L.; Ford, D.; Hirst, B. H. P-Glycoprotein Potentiates Cyp3A4-Mediated Drug Disappearance During Caco-2 Intestinal Secretory Detoxification. *J. Drug Targeting* **2004**, *12*, 405–413.

(42) Christians, U.; Schmitz, V.; Haschke, M. Functional Interactions between P-Glycoprotein and Cyp3A in Drug Metabolism. *Expert Opin. Drug Metab. Toxicol.* **2005**, *1*, 641–654.

(43) Mouly, S. J.; Paine, M. F.; Watkins, P. B. Contributions of Cyp3A4, P-Glycoprotein, and Serum Protein Binding to the Intestinal First-Pass Extraction of Saquinavir. *J. Pharmacol. Exp. Ther.* **2004**, *308*, 941–948.

(44) Tam, D.; Sun, H.; Pang, K. S. Influence of P-Glycoprotein, Transfer Clearances, and Drug Binding on Intestinal Metabolism in Caco-2 Cell Monolayers or Membrane Preparations: A Theoretical Analysis. *Drug Metab. Dispos.* **2003**, *31*, 1214–1226.

(45) Sun, H.; Chow, E. C.; Liu, S.; Du, Y.; Pang, K. S. The Caco-2 Cell Monolayer: Usefulness and Limitations. *Expert Opin. Drug Metab. Toxicol.* **2008**, *4*, 395–411.

$$\mathrm{ER} = \frac{\sum \text{metabolites}}{\sum \text{metabolites} + P_{\text{receiver}}} \quad (3)$$

Benet and colleagues added the amount of drug in the cell (P_{cell}) to the denominator of eq 3 and redefined ER as[38−40]

$$\mathrm{ER} = \frac{\sum \text{metabolites}}{\sum \text{metabolites} + P_{\text{receiver}} + P_{\text{cell}}} \quad (4)$$

Both eqs 3 and 4 fail to consider the amount of drug in the donor compartment (P_{donor}). Pang's group, recognizing that the drug in the donor and receiver compartments is able to re-enter the cell and be metabolized, suggested use of the fraction of dose metabolized.[32,44,45]

$$\text{fraction of dose metabolized } (f_{\text{met}}) = \frac{\sum \text{metabolites}}{\sum \text{metabolites} + P_{\text{receiver}} + P_{\text{cell}} + P_{\text{donor}}} \quad (5)$$

The metabolite/parent ratio (eq 2) and the ERs in eqs 3 and 4 are unable to account for the aggregate metabolism in the system because the amounts of drug in the cell and donor (apical or basolateral) compartments are absent despite that these are available for entry into the cell and therefore metabolism. The ER is not a true extraction ratio since the drug amount in the donor compartment is unaccounted for, and the drug can reenter the cell for metabolism in this closed system, rendering the parameter inadequate to describe the extent of metabolism. Hence f_{met} (eq 5) is the better parameter to express the extent of metabolism in this closed system.

Caco-2 Modeling. Sun and Pang employed the catenary model that contains the donor, cell, and receiver compartments (Figure 2) to examine the requisite processes of transport and metabolism that influence the apparent permeabililty.[32] The solutions for $P_{\text{app(B}\rightarrow\text{A)}}$ and $P_{\text{app(A}\rightarrow\text{B)}}$ obtained from matrix inversion, were too lengthy to be presented. But a concise solution was obtained for EfR under linear conditions that revealed the influence of the transport and metabolic parameters.[32]

$$\mathrm{EfR} = \frac{f_{\text{baso}}(CL_{d1} + CL_{\text{in}})(CL_{\text{int,sec}} + CL_{d4})}{f_{\text{ap}}(CL_{d2} + CL_{\text{ef}})(CL_{\text{abs}} + CL_{d3})} \quad (6)$$

The above equation shows that the EfR is not influenced by the metabolic intrinsic clearance ($CL_{\text{int,met}}$) or unbound fraction in the cell (f_{cell}) under first-order conditions, and that, in the absence of carrier mediated transport at the basolateral membrane and transporters for apical absorption ($CL_{\text{in}} = Cl_{\text{ef}} = CL_{\text{abs}} = 0$) as well as drug binding in the basolateral and apical compartments ($f_{\text{baso}} = f_{\text{ap}} = 1$), the equation is simplified when $CL_{d1} = CL_{d2}$ and $CL_{d3} = CL_{d4}$.

$$\mathrm{EfR} = \frac{CL_{\text{int,sec}}}{CL_{d4}} + 1 \quad (7)$$

Then what is the mechanism to explain the data? Which camp is correct in reviewing transporter−enzyme interplay? To thoroughly investigate this problem, Fan et al. performed simulations pertaining to the Caco-2 problem under both linear and nonlinear conditions, and the fraction metabolized (f_{met}), ER, and EfR were estimated.[46] The simulations, based on sampling at the 30, 60, 90, or 120 min time point, revealed that both the f_{met} (Figure 3A) and ER (Figure 3B) that displayed different values among the time points showed similar trends when $CL_{\text{int,sec}}$ was increased, regardless of the passive permeability (CL_d); however, the patterns were asymmetrical with respect to the dosing site (apical or basolateral) due to the different volumes of the apical and basolateral compartments in the Transwell system. The MRT was increased under linear conditions, as was EfR which increased proportionally with $CL_{\text{int,sec}}$ (Figure 3C) and was insensitive to changes in the metabolic activities ($CL_{\text{int,met}}$), as found by Sun and Pang.[32] The increased secretory activity ($CL_{\text{int,sec}}$) led to decreased metabolism (f_{met}) and reduced ER[46] despite the longer MRT, and conformed to the reciprocal relation or seesaw phenomenon predicted based on the competition for the substrate within the cell.

For simulations performed under nonlinear metabolic conditions, the MRT again increased with $CL_{\text{int,sec}}$.[46] Asymmetrical and decreasing trends resulted for the f_{met} regardless of dosing into the apical or basolateral compartment, and again the time of sampling provided different values, and a greater sensitivity was observed with lower CL_{abs} values (Figure 4A, cf. upper and lower panels), since a higher CL_{abs} evoked a higher degree of saturation. Values of f_{met} persisted to display a reciprocal relationship with $CL_{\text{int,sec}}$ (Figure 4A). The ER pattern, on the other hand, showed route-dependent patterns, revealing a decreasing trend with increasing $CL_{\text{int,sec}}$ for basolateral dosing but an increasing profile with apical administration (Figure 4B). The observed data could be explained for the case of saturable metabolism, since, upon re-entry of the apically secreted drug from the apical compartment into the cell, the drug would encounter a more desaturated enzyme system, and the "apparent" ER estimate would increase.[42,44−46] The EfR values tended to increase with $CL_{\text{int,sec}}$, though not as much as for linear conditions (Figure 4C).

From these composite observations for linear and nonlinear metabolic conditions, it can be concluded that the sampling times did affect values of the MRT, f_{met}, ER and EfR, but not the patterns of change with $CL_{\text{int,sec}}$. The MRT increases with increased secretion; f_{met} displays a reciprocal or seesaw relationship with secretion. But the parameter ER is not consistent with changes in secretion under saturable metabolic conditions, and is route-dependent. The inability of ER to delineate the extent of metabolism is due to its limited definition that neglects to account for drug in the donor compartment. For compounds that are highly secreted into

(46) Fan, J.; Maeng, H. J.; Pang, K. S. Interplay of Transporters and Enzymes in the Caco-2 Cell Monolayer. I. Effect of Altered Apical Secretion. Submitted.

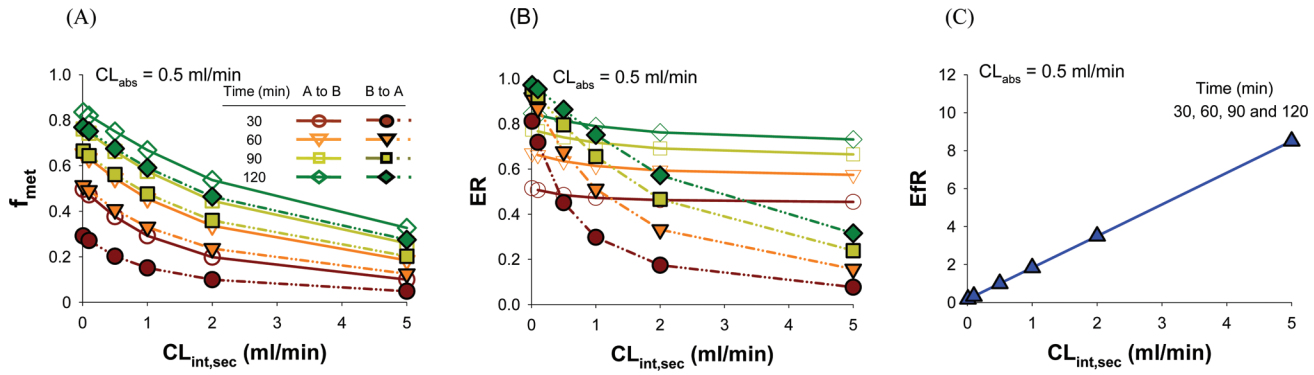

Figure 3. Effects of $CL_{int,sec}$ on the fraction of dose metabolized, f_{met}, according to eq 5 (A), ER according to eq 4 (B), and EfR (C) under linear conditions in the Caco-2 system. Different sampling times of 30 (red round circles), 60 (orange inverted triangles), 90 (light green squares) and 120 (deep green diamonds) min for the A → B (solid lines) and B → A (dashed lines) directions were simulated based on CL_{abs} = 0.5 mL/min, $CL_{int,met}$ = 0.05 mL/min, CL_{d1} = CL_{d2} = 0.1 mL/min, CL_{in} = CL_{ef} = 0. The patterns were very similar to those repeated for CL_{abs} = 0.1 and 1 mL/min and for CL_{d1} = CL_{d2} = 0.05 or 0.5 mL/min; when $CL_{int,met}$ was 0.5 mL/min, changes in f_{met} and ER were much smaller with increasing $CL_{int,sec}$ (reproduced from reference 46, with permission).

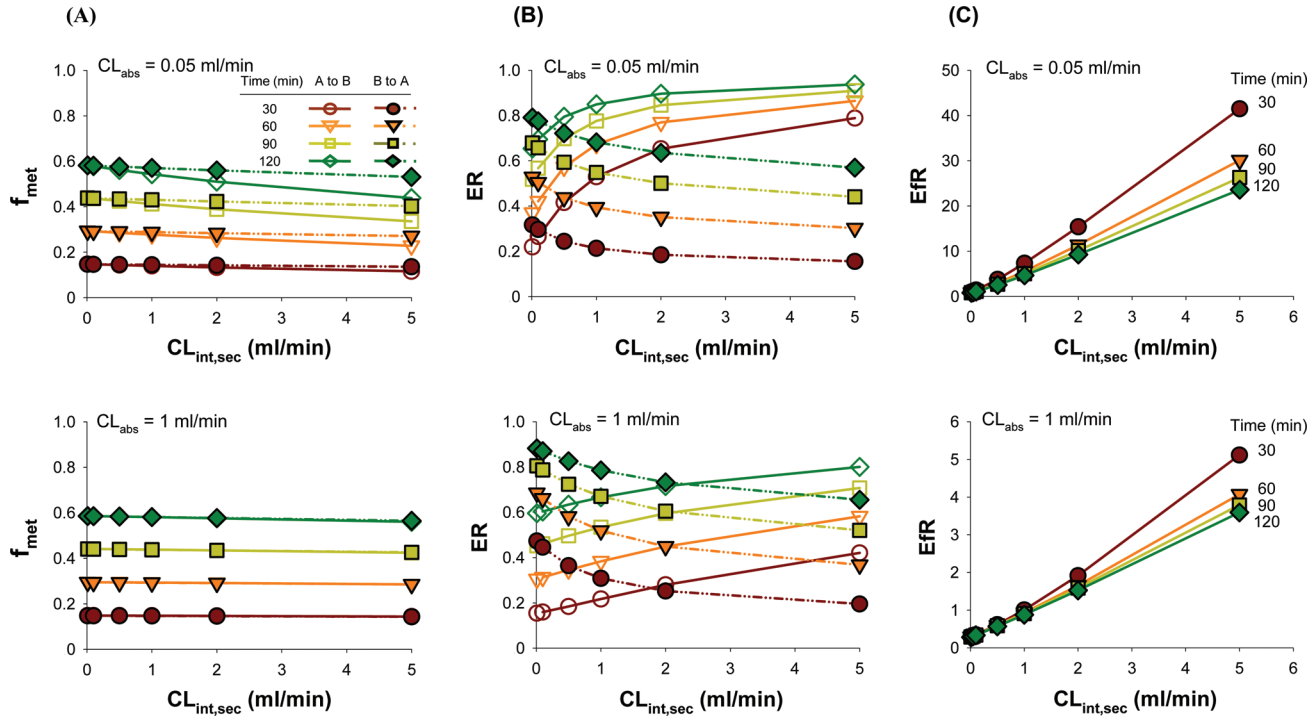

Figure 4. Effects of $CL_{int,sec}$ on the fraction of dose metabolized, f_{met} according to eq 5 (A), ER according to eq 4 (B), and EfR (C) under nonlinear conditions of metabolism (V_{max} = 0.5 nmol/min and K_m = 0.5 μM) in the Caco-2 cell system. Data were simulated at sampling times of 30 (red round circles), 60 (orange inverted triangles), 90 (light green squares) and 120 (deep green diamonds) min for the A → B (solid line) and B → A (stippled line) directions based on CL_{abs} = 0.05 or 1 mL/min, CL_{d1} = CL_{d2} = 0.1 mL/min, CL_{in} = CL_{ef} = 0. The patterns were very similar for CL_{d1} = CL_{d2} = 0.05 or 0.5 mL/min (reproduced from reference 46, with permission).

the apical compartment and are able to re-enter the cell for metabolism, the ER will underestimate the extent of drug metabolism, especially for apical (donor compartment) dosing. The unusual, increasing pattern of ER with increasing $CL_{int,sec}$ is attributed mostly to nonlinear metabolism (Figure 4B), and can also be due to events of saturable basolateral influx.[46] These results confirm that f_{met} rather than ER is the more appropriate parameter to express the extent of metabolism.[32,44−46] The f_{met} is a better index to reflect the metabolism in transporter−enzyme interplay. This view is supported by Knight et al.[47]

Examples. Data of several studies that investigated the interplay between P-gp and CYP3A were re-examined. Mostly, eq 4 or eq 3 was used in the calculation of ER. Whenever data was available, we estimated P_{donor} from the data with the program GetData (ShareIt!, Germany) to arrive

Table 1. Summary of Changes in Metabolism with P-gp Inhibitors in the Cell Monolayer in Culture (See Figures 3 and 4 for the Deduced Trends)

Drug	P-gp Inhibitors	Observations	Explanation	References
Indinavir (5 μM) in 1α,25-dihydroxyvitamin D_3 treated Caco-2 cells	+ Cyclosporin A (5 μM); only for P-gp inhibition	• $\downarrow ER_{(A\rightarrow B)Eq.2}$ and $\downarrow ER_{(B\rightarrow A)Eq.2}$ • $f_{met\,(A\rightarrow B)}$ and $f_{met(B\rightarrow A)}$ increased with cyclosporin without cyclosporin: $f_{met(A\rightarrow B)} = 0.014$; $f_{met(B\rightarrow A)} = 0.011$ with cyclosporin: $f_{met(A\rightarrow B)} = 0.018$; $f_{met(B\rightarrow A)} = 0.016$	Inhibition of P-gp by cyclosporine increased f_{met} in both A and B dosing, as predicted by Figs. 3A and 4A; P-gp inhibition promoted higher drug concentration in cell for metabolism	37
K77 (10 μM) in CYP3A4 transfected Caco-2 cells	+ GF120918 (200 nM)	• $\downarrow ER_{(A\rightarrow B)Eq.4}$ and $\uparrow ER_{(B\rightarrow A)Eq.4}$ • $f_{met(A\rightarrow B)}$ and $f_{met(B\rightarrow A)}$ increased with GF120918 without GF120918: $f_{met(A\rightarrow B)} = 0.021$; $f_{met(B\rightarrow A)} = 0.0078$ with GF120918: $f_{met(A\rightarrow B)} = 0.032$; $f_{met(B\rightarrow A)} = 0.011$	Inhibition of P-gp by GF120918 increased f_{met} in both A and B dosing, as predicted by Figs. 3A and 4A[a]; P-gp inhibition promoted higher drug concentration in cell for metabolism	38
Sirolimus (1 μM) in CYP3A4 transfected Caco-2 cells	+GF120918 (200 nM)	• $\downarrow ER_{(A\rightarrow B)Eq.4}$ and $\uparrow ER_{(B\rightarrow A)Eq.4}$ • $f_{met(A\rightarrow B)}$ and $f_{met(B\rightarrow A)}$ decreased and reason was unknown	Explained by Figure 4B with decreased $CL_{int,sec}$	39
Erythromycin and vinblastine (50 μM) in 1α,25-dihydroxyvitamin D_3 treated Caco-2 cells	+Digoxin (100 μM)	• $\downarrow f_{met(B\rightarrow A)}$; and $f_{met(A\rightarrow B)}$ unchanged	Explained partially by Figure 4B with decreased $CL_{int,sec}$	41
Saquinavir (40 μM) in 1α,25-dihydroxyvitamin D_3 treated Caco-2 cells	+ LY335959 (0.5 μM)	• $\downarrow ER_{(A\rightarrow B)Eq.3}$ • $\uparrow f_{met(A\rightarrow B)}$ and $f_{met(B\rightarrow A)}$ increased with LY335959 without LY335959: $f_{met(A\rightarrow B)} = 0.012$; $f_{met(B\rightarrow A)} = 0.0016$ with LY335959: $f_{met(A\rightarrow B)} = 0.0029$; $f_{met(B\rightarrow A} = 0.0033$	Inhibition of P-gp by LY335959 increased f_{met} in both A and B dosing, as predicted by Figs. 3A and 4A; P-gp inhibition promoted higher drug concentration in cell for metabolism	43

[a] Contrary to this view of saturable metabolism, no issue of nonlinearity in metabolism was found according to Cummins et al.[38]

at the changes in f_{met} according to eq 5 (Table 1). Figures 3 and 4 were also used to interpret the changes in the f_{met} and ER upon reduction in $CL_{int,sec}$ in the presence of P-gp inhibitors. K77 (a novel cysteine protease inhibitor), which is a dual CYP3A4 and P-gp substrate, was used to study enzyme and transporter interplay in cultured cells in the presence of GF120918,[38] a P-gp inhibitor. The data showed that the calculated f_{met} was increased in the presence of the P-gp inhibitors, displaying the seesaw phenomenon expected of increased metabolism with decreased secretion. Similar trends were observed with sirolimus,[39] erythromycin, and vinblastine,[41] showing that the calculated f_{met} was increased in the presence of the P-gp inhibitors though the ER estimated according to eq 4 was decreased for A → B dosing (Table 1). We surmise that metabolism must have become saturated for these examples. Saquinavir, a potent HIV protease inhibitor that undergoes CYP3A4-mediated metabolism to form monohydroxylated compounds with a high intrinsic metabolic clearance in microsomes and Caco-2 cells[48,49] and revealed a high efflux ratio of saquinavir (6.4) in Caco-2 cells due to P-gp[50] but not MRP2 efflux.[51] In the presence of LY335979 (P-gp inhibitor), a higher ER was found,[43] and f_{met} increased upon P-gp inhibition after apical administration, fully demonstrating the seesaw phenomenon between secretion transporters and metabolic enzymes. When indinavir, the HIV protease inhibitor, was evaluated for the interaction between intestinal CYP3A4[52,53] and P-gp in Caco-2 cells,[54,55] oxidation of indinavir by CYP3A4 occurred with a K_m of 8.1 μM and V_{max} of 1.54×10^{-4} nmol·min^{-1}·mg protein^{-1}, with M6, the product from N-depyridomethylation being the most prominent metabolite formed.[37] The total amount of M6 formed from indinavir after 4 h of incubation in Caco-2 cells was significantly increased for apical-to-basolateral direction and basolateral-

(47) Knight, B.; Troutman, M.; Thakker, D. R. Deconvoluting the Effects of P-Glycoprotein on Intestinal Cyp3A: A Major Challenge. *Curr. Opin. Pharmacol.* **2006**, *6*, 528–532.

(48) Eagling, V. A.; Wiltshire, H.; Whitcombe, I. W.; Back, D. J. Cyp3A4-Mediated Hepatic Metabolism of the HIV-1 Protease Inhibitor Saquinavir in Vitro. *Xenobiotica* **2002**, *32*, 1–17.

(49) Fitzsimmons, M. E.; Collins, J. M. Selective Biotransformation of the Human Immunodeficiency Virus Protease Inhibitor Saquinavir by Human Small-Intestinal Cytochrome P4503A4: Potential Contribution to High First-Pass Metabolism. *Drug Metab. Dispos.* **1997**, *25*, 256–266.

(50) Foger, F.; Kafedjiiski, K.; Hoyer, H.; Loretz, B.; Bernkop-Schnurch, A. Enhanced Transport of P-Glycoprotein Substrate Saquinavir in Presence of Thiolated Chitosan. *J. Drug. Targeting* **2007**, *15*, 132–139.

(51) Usansky, H. H.; Hu, P.; Sinko, P. J. Differential Roles of P-Glycoprotein, Multidrug Resistance-Associated Protein 2, and Cyp3A on Saquinavir Oral Absorption in Sprague-Dawley Rats. *Drug Metab. Dispos.* **2008**, *36*, 863–869.

(52) Balani, S. K.; Woolf, E. J.; Hoagland, V. L.; Sturgill, M. G.; Deutsch, P. J.; Yeh, K. C.; Lin, J. H. Disposition of Indinavir, a Potent HIV-1 Protease Inhibitor, after an Oral Dose in Humans. *Drug Metab. Dispos.* **1996**, *24*, 1389–1394.

(53) Chiba, M.; Hensleigh, M.; Nishime, J. A.; Balani, S. K.; Lin, J. H. Role of Cytochrome P450 3A4 in Human Metabolism of MK-639, a Potent Human Immunodeficiency Virus Protease Inhibitor. *Drug Metab. Dispos.* **1996**, *24*, 307–314.

(54) Kim, R. B.; Fromm, M. F.; Wandel, C.; Leake, B.; Wood, A. J.; Roden, D. M.; Wilkinson, G. R. The Drug Transporter P-Glycoprotein Limits Oral Absorption and Brain Entry of HIV-1 Protease Inhibitors. *J. Clin. Invest.* **1998**, *101*, 289–294.

to-apical direction with cyclosporin A (a CYP3A4 and P-gp inhibitor) at 30 μM, a concentration that is devoid of inhibitory effects on metabolism.[37] With cyclosporin A acting solely as a P-gp inhibitor in this case, the amount of indinavir transported in the apical-to-basolateral direction was increased, and the total amount of M6 formed at 4 h (upon summation of data presented in Figure 3 of Hochman et al.[37] with GetData) was also significantly increased for both apical and basolateral dosing. However, the distribution of M6 was significantly shifted from the apical compartment to greater abundances in cellular and basolateral compartments in the presence of the P-gp inhibitor,[37] suggesting that M6 is also a P-gp substrate. The accumulation of M6 within the cell in the presence of cyclosporin A failed to alter indinavir metabolism, but the resulting metabolite may compete with indinavir for P-gp. Nevertheless, the reciprocal relation or seesaw phenomenon on increased metabolism with decreased secretion was again observed here.

In closed systems not dissimilar to the Caco-2 cell monolayer, Johnson et al. observed, at increasing verapamil concentrations in the mounted rat jejunal tissue chamber, an increased cellular residence time of verapamil in the mucosal to serosal direction relative to the serosal to mucosal direction (3×), and a 2-fold increase in metabolism to form norverapamil and the D-617 metabolite.[56] However, nonlinear metabolism and secretion had prevailed at higher concentrations and clouded the interpretation of MRT, a first-order concept. Then Johnson et al. studied the fate of verapmail in the luminal-autoperfused rat jejunal segment in the presence of PSC833 (P-gp inhibitor), midazolam (CYP3A inhibitor), and ketoconazole (P-gp and P450 inhibitor).[57] While both the control and inhibition data were well predicted by the compartmental model, the extraction ratio (ER), defined as the ratio of the metabolic rate constant/(sum of metabolic and secretion rate constants), seemed to be more consistent with eq 3 by Fisher et al.[36] than eq 4 of Cummins et al.[38−40] and showed a decrease ER with P-gp inhibition by PSC833. Upon estimation with GetData, f_{met} (eq 5) was predicted to increase with PSC833 inhibition of P-gp, indicative of the seesaw phenomenon that is predicted by Figures 3 and 4. Again, Johnson's definition of the ER as the ratio of metabolic/(metabolic + secretion) is not a true parameter in the sense of an extraction ratio, since there is equilibrium from the mucosal and serosal with the cellular compartment.[57] Lastly, in a diffusion chamber used for the examination of *in vitro* permeability, Johnson et al.[58] also examined the metabolism and secretion of verapamil by Cyp3a and P-gp in the presence and absence of the inhibitors, midazolam, ketoconazole, and PSC833. However, no change in metabolism was observed with P-gp inhibitors.

The above examples in the Caco-2 monolayer showed that f_{met} is the parameter that consistently displayed reciprocal (or seesaw) relationships with increased apical secretion and Figures 3 and 4 may be routinely used to fully explain the interplay between transporters and enzymes under both linear and nonlinear conditions of metabolism.

V. Transporter−Enzyme Interplay in the Liver

Both the P-gp and the CYP3A enzyme are highly expressed in liver.[27] Since many drugs are common substrates of the P-gp and CYP3A, transporter−enzyme interplay or drug−drug interaction is not an uncommon occurrence.[59] The nature of competition is not restricted to the interaction between enzymes and transporter but exists between enzyme and enzyme and transporter and transporter. Morris and Pang[60] commented that the induction of one pathway would lead to reduction in clearance or rate of the alternate, competing metabolic pathway. Sirianni and Pang[30] appraised the interplay between the excretory transporter and enzyme in the liver, as did Liu and Pang,[1,61] and asserted that increased secretory transporter activity should decrease the rate of metabolism under linear kinetic conditions. The underlying reason is the competition for the intracellular substrate concentration. Reports have been mostly based on observations originating from liver perfusion studies, isolated hepatocytes, cell lines, sandwich systems, and knockout animals. Some of these early accounts suggest that inhibition of P-gp leads to increased metabolism in hepatocytes. It was reported that internalization of Mrp2, Bsep, and P-gp[62−64] exists for freshly prepared hepatocytes. The internalized P-gp may lead to accumulation of drug within the hepatocyte. The

(55) Lee, C. G.; Gottesman, M. M.; Cardarelli, C. O.; Ramachandra, M.; Jeang, K. T.; Ambudkar, S. V.; Pastan, I.; Dey, S. HIV-1 Protease Inhibitors Are Substrates for the Mdr1 Multidrug Transporter. *Biochemistry* **1998**, *37*, 3594–3601.

(56) Johnson, B. M.; Charman, W. N.; Porter, C. J. H. The Impact of P-Glycoprotein Efflux on Enterocyte Residence Time and Enterocyte-Based Metabolism of Verapamil. *J. Pharm. Pharmacol.* **2001**, *53*, 1611–1619.

(57) Johnson, B. M.; Chen, W.; Borchardt, R. T.; Charman, W. N.; Porter, C. J. H. A Kinetic Evaluation of the Absorption, Efflux, and Metabolism of Verapamil in the Autoperfused Rat Jejunum. *J. Pharmacol. Exp. Ther.* **2003**, *305*, 151–158.

(58) Johnson, B. M.; Charman, W. N.; Porter, C. J. Application of Compartmental Modeling to an Examination of in Vitro Intestinal Permeability Data: Assessing the Impact of Tissue Uptake, P-Glycoprotein, and Cyp3A. *Drug Metab. Dispos.* **2003**, *31*, 1151–1160.

(59) Pal, D.; Mitra, A. K. Mdr- and Cyp3A4-Mediated Drug-Drug Interactions. *J. Neuroimmune Pharmacol.* **2006**, *1*, 323–339.

(60) Morris, M. E.; Pang, K. S. Competition between Two Enzymes for Substrate Removal in Liver: Modulating Effects Due to Substrate Recruitment of Hepatocyte Activity. *J. Pharmacokinet. Biopharm.* **1987**, *15*, 473–496.

(61) Liu, L.; Pang, K. S. An Integrated Approach to Model Hepatic Drug Clearance. *Eur. J. Pharm. Sci.* **2006**, *29*, 215–230.

(62) Sekine, S.; Ito, K.; Horie, T. Oxidative Stress and Mrp2 Internalization. *Free Radical Biol. Med.* **2006**, *40*, 2166–2174.

(63) Perez, L. M.; Milkiewicz, P.; Elias, E.; Coleman, R.; Sanchez Pozzi, E. J.; Roma, M. G. Oxidative Stress Induces Internalization of the Bile Salt Export Pump, Bsep, and Bile Salt Secretory Failure in Isolated Rat Hepatocyte Couplets: A Role for Protein Kinase C and Prevention by Protein Kinase A. *Toxicol. Sci.* **2006**, *91*, 150–158.

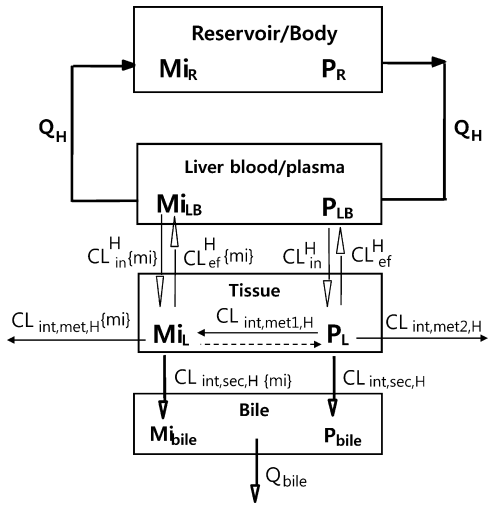

Figure 5. Physiologically based pharmacokinetic (PBPK) model of the liver, the only elimination organ. The model is divided into four compartments: the reservoir (R), liver blood (LB), liver (L) and bile compartment (bile). The influx (CL^H_{in}) and efflux (CL^H_{ef}) clearances at the basolateral membrane denote entry and exit of the parent drug (P) or metabolite (Mi) between blood and liver tissue. Only the unbound drug or metabolite undergoes transport and metabolism, but the unbound fractions are not shown graphically in the figure to retain clarity, though these are considered in the rate equations. Metabolism and excretion into bile occur with the metabolite formation intrinsic clearance, $CL_{int,met1,H}$ for the assigned metabolite Mi_L, or $CL_{int,met2,H}$ for alternate metabolites and biliary intrinsic clearance, $CL_{int,sec,H}$, respectively. Hepatic blood flow rate and bile flow rate are denoted by Q_H and Q_{bile}, respectively. Metabolite parameters are further qualifed by "{mi}". For futile cycling, the backward, interconversion intrinsic clearance of the metabolite [$CL^{Mi\rightarrow D}_{int,met}\{mi\}$] to reform the drug was shown by the dashed line, and the forward formation clearance of the metabolite, shown as $CL_{int,met1,H}$ in the figure, was replaced by $CL^{D\rightarrow Mi}_{int,met}$ (modified from refs 4 and 68, with permission).

complication renders interpretation of AUC changes to be more difficult for isolated hepatocytes.

PBPK Modeling of the Liver. The best discriminatory method to examine the interplay is via modeling and simulations. PBPK modeling of the liver, based on the liver as the only eliminating organ, is a well developed concept. The model for the recirculating perfused liver system consisted of four compartments: the reservoir (R, or blood compartment), liver blood (LB), liver tissue (L), and bile compartment (bile) is used (Figure 5). The blood flow rate and protein binding are denoted by Q_H for liver blood, f_B for unbound fraction in blood, and f_L for unbound fraction in liver, respectively. The transport processes underlying carrier-mediation or passive diffusion are summed and represented by the influx and efflux clearances (CL^H_{in} and CL^H_{ef}). The model includes the formation pathway of the metabolite, Mi, with the formation intrinsic clearance, $CL_{int,met1,H}$, and metabolism ($CL_{int,met2,H}$) and excretion ($CL_{int,sec,H}$) as the alternate elimination pathways for the drug. Since metabolite data is very informative of enzyme−transporter interplay, the metabolite AUC [AUC{mi,P}] should also be solved, after accommodation of elimination pathways of the formed metabolite in the PBPK model.[4] The metabolite in the liver (Mi_L) further undergoes metabolism with the intrinsic metabolic clearance, $CL_{int,met,H}\{mi\}$, or is excreted into bile with the intrinsic secretory clearance $CL_{int,sec,H}\{mi\}$; the influx and efflux of metabolite are denoted by $CL^H_{in}\{mi\}$ and $CL^H_{ef}\{mi\}$, respectively, and binding is described by $f_B\{mi\}$ in blood and $f_L\{mi\}$ in liver.

As shown in Table 2, the AUC of drug after intravenous dosing (AUC_{iv}) is a complex equation related to the blood flow rate (Q_H), unbound fraction in blood (f_B), influx (CL^H_{in}) and efflux (CL^H_{ef}) uptake clearances, and the total hepatic intrinsic clearance ($CL_{int,H}$). It is notable that the $AUC_{iv}\{mi,P\}$ is dependent on its formation intrinsic clearance, $CL_{int,met1,H}$, and individual components of the total $CL_{int,H}$ or $CL_{int,met1,H}$, $CL_{int,met2,H}$, and $CL_{int,sec,H}$, as well as vascular binding and the transport ($CL^H_{in}\{mi\}$ and $CL^H_{ef}\{mi\}$) and the intrinsic $CL_{int,H}\{mi\}$ clearance of the metabolite. In the case of a drug with flow-limited distribution (i.e., when $CL^H_{in} \cong CL^H_{ef} \gg Q_H$), these equations are simplified (Table 2).

The equations provide meaningful insight to illustrate the competing nature between transporters and enzymes in liver. With the equations shown in Table 2, patterns of change may be obtained upon perturbation in the metabolic, influx, efflux, or metabolic as well as secretory intrinsic clearances on the predicted clearances. Table 3 shows the general trends predicted by the PBPK liver model (equations in Table 2) under linear conditions. These trends are consistent with those from previous simulation studies.[1,61] For example, an increase in one elimination pathway such as secretion (or metabolism) would increase the clearance of the pathway but decrease clearance of the alternate pathway, increasing the total clearance and decreasing the AUC_{iv} (Figures 6A and 6B). Generally speaking, inhibition of the formation pathway ($CL_{int,met1,H}$) results in higher AUC_{iv} and higher clearances of the alternate pathways, but a smaller area under the curve of the formed metabolite, $AUC_{iv}\{mi,P\}$, and reduced metabolite formation clearance ($CL_{H,met1}$) and total hepatic drug clearance (CL_H) (Figures 6A and 6C). Conversely, an increase in $CL_{int,met1,H}$ leads to decreased AUC_{iv} and $CL_{H,ex}$ or $CL_{H,met2}$ but higher $AUC_{iv}\{mi,P\}$, $CL_{H,met1}$ and CL_H (Figures 6A and 6C). By contrast, an increase in $CL_{int,met2,H}$ leads to decreased AUC_{iv} and $CL_{H,ex}$ or $CL_{H,met1}$ and lower $AUC_{iv}\{mi,P\}$, $CL_{H,met1}$ and higher CL_H (Figures 6B and D). An increase of $CL_{int,sec,H}$ would lead to an increase in $CL_{H,ex}$ and CL_H but decreased $CL_{H,met1}$ and $CL_{H.met2}$ and

(64) Bow, D. A.; Perry, J. L.; Miller, D. S.; Pritchard, J. B.; Brouwer, K. L. Localization of P-gp (Abcb1) and Mrp2 (Abcc2) in Freshly Isolated Rat Hepatocytes. *Drug Metab. Dispos.* **2008**, *36*, 198–202.

Table 2. Equations Denoting the Area under the Curve (AUC) and Total Hepatic Clearance (CL_H)[a]

Parameters	With barrier	Without barrier (Flow limited distribution)
AUC_{iv}	$\frac{Dose_{iv}\left[Q_H(CL_{ef}^H + CL_{int,H}) + f_B CL_{in}^H CL_{int,H}\right]}{f_B CL_{in}^H Q_H CL_{int,H}}$	$\frac{Dose_{iv}\left[(Q_H + f_B CL_{int,H})\right]}{Q_H f_B CL_{int,H}}$
$AUC_{iv}\{mi,P\}$	$\frac{Dose_{iv} CL_{int,met1,H} CL_{ef}^H\{mi\}}{(CL_{int,met1,H} + CL_{int,met2,H} + CL_{int,sec,H}) f_B\{mi\} CL_{in}^H\{mi\} CL_{int,H}\{mi\}}$	$\frac{Dose_{iv} CL_{int,met1,H}}{(CL_{int,met1,H} + CL_{int,met2,H} + CL_{int,sec,H}) f_B\{mi\} CL_{int,H}\{mi\}}$
CL_H (Total Hepatic Clearance)	$Q_H \frac{f_B CL_{int,H} CL_{in}^H}{Q_H CL_{ef}^H + CL_{int,H}(Q_H + f_B CL_{in}^H)}$	$\frac{Q_H f_B CL_{int,H}}{Q_H + f_B CL_{int,H}}$
$CL_{H,met1}$ (Formation Clearance of Mi)	$Q_H \frac{f_B CL_{int,met1,H} CL_{in}^H}{Q_H CL_{ef}^H + CL_{int,H}(Q_H + f_B CL_{in}^H)}$	$\frac{Q_H f_B CL_{int,met1,H}}{(Q_H + f_B CL_{int,H})}$
$CL_{H,met2}$ (Metabolic Clearance for Formation of Other Metabolites)	$Q_H \frac{f_B CL_{int,met2,H} CL_{in}^H}{Q_H CL_{ef}^H + CL_{int,H}(Q_H + f_B CL_{in}^H)}$	$\frac{Q_H f_B CL_{int,met2,H}}{(Q_H + f_B CL_{int,H})}$
$CL_{H,ex}$ (Biliary Clearance of Drug)	$Q_H \frac{f_B CL_{int,sec,H} CL_{in}^H}{Q_H CL_{ef}^H + CL_{int,H}(Q_H + f_B CL_{in}^H)}$	$\frac{Q_H f_B CL_{int,sec,H}}{(Q_H + f_B CL_{int,H})}$

[a] Reprinted with permission from ref 4. Copyright 2008 K. Sandy Pang, Marilyn E. Morris and Huadong Sun.

Table 3. General Trends in the Metabolic, Excretion, and Total Hepatic Clearance upon Changes in the Influx, Efflux, Metabolic, or Secretory Intrinsic Clearances under Linear Conditions for the PBPK Model (Reciprocal Concept or Seesaw Phenomenon)

	$CL_{H,met1}$ Metabolite Formation Clearance	$CL_{H,met2}$ Clearance for Alternate Metabolism	$CL_{H,,ex}$ Biliary Clearance	CL_H Total Hepatic Clearance
$\uparrow CL_{in}^H$ / $\downarrow CL_{ef}^H$	↑	↑	↑	↑
$\downarrow CL_{in}^H$ / $\uparrow CL_{ef}^H$	↓	↓	↓	↓
$\uparrow CL_{int,met1,H}$ / $\downarrow CL_{int,met1,H}$	↑ / ↓	↓ / ↑	↓ / ↑	↑ / ↓
$\uparrow CL_{int,met2,H}$ / $\downarrow CL_{int,met2,H}$	↓ / ↑	↑ / ↓	↓ / ↑	↑ / ↓
$\uparrow CL_{int,sec,H}$ / $\downarrow CL_{int,sec,H}$	↓ / ↑	↓ / ↑	↑ / ↓	↑ / ↓

lower AUC_{iv} and $AUC_{iv}\{mi,P\}$ (Figure 6). The simulations fully demonstrate the competing nature of transporters and enzymes, and show clearly that metabolism contributes to an underestimation of the apparent, excretory clearance and vice versa (Figure 6). Accordingly, the interplay between enzymes and canalicular efflux transporters is a seesaw phenomenon,[1,30] since both enzymes and canalicular efflux transporters compete for the intracellular substrate for elimination.

PBPK Modeling of the Liver with Futile Cycling. PBPK modeling of the liver for a drug and metabolite undergoing futile cycling has recently been performed.[65,66] This PBPK model has an additional, unusual pathway over that shown in Figure 5. Within the hepatocyte, the precursor drug (D_L) is metabolized to its interconversion metabolite in the liver tissue (Mi_L) by the metabolic intrinsic clearance $CL_{int,met}^{D\rightarrow Mi}$ (defined as $CL_{int,met1,H}$ in Figure 5), and an additional pathway exists for backward conversion of the metabolite Mi_L to reform the parent drug in the liver D_L with the intrinsic clearance, $CL_{int,met}^{Mi\rightarrow D}\{mi\}$ (absent normally, shown as dashed line in Figure 5).

The AUCs of the drug and metabolite in the reservoir (subscript, R) and liver (subscript, L) and cumulative biliary excretion of drug and metabolite ($A_{e,\infty}$ and $A_{e,\infty}\{mi\}$) solved for the model (Table 4) are similar in form to those presented in Table 2 when futile cycling is absent.[30] The exception is that two additional terms, ef_m'' and ef_m', are now present. These terms are needed to describe the modulation of the backward and forward processes in futile cycling, respectively, on the net metabolism of the precursor drug and metabolite. The term ef_m'' or $(CL_{int,sec,H}\{mi\} + CL_{int,met}^{other}\{mi\})/(CL_{int,sec,H}\{mi\} + CL_{int,met}^{Mi\rightarrow D}\{mi\} + CL_{int,met}^{other}\{mi\})$, or effective coefficient for metabolite formation, is found as a product with the metabolite formation, intrinsic clearance $CL_{int,met}^{D\rightarrow Mi}$ (equivalent to $CL_{int,met1,H}$ in Figure 5), and relates to intrinsic clearance terms associated with the metabolite: the intrinsic clearance denoting reformation of the precursor $CL_{int,met}^{Mi\rightarrow D}\{mi\}$ as well as other terms for secretion ($CL_{int,sec,H}\{mi\}$) and sequential metabolism ($CL_{int,met}^{other}\{mi\}$) of the metabolite. The second term, ef_m' or $(CL_{int,sec,H} + CL_{int,met}^{other})/(CL_{int,sec,H} + CL_{int,met}^{D\rightarrow Mi} + CL_{int,met}^{other})$, or the effective recycling coefficient, is found as a product with the metabolic intrinsic clearance of metabolite to reform the precursor $CL_{int,met}^{Mi\rightarrow D}\{mi\}$, and appears in the denominator of the solution of $AUC_R\{mi,P\}$ and

(65) Sun, H.; Liu, L.; Pang, K. S. Increased Estrogen Sulfation of Estradiol 17β-D-Glucuronide in Metastatic Tumor Rat Livers. *J. Pharmacol. Exp. Ther.* **2006**, *319*, 818–831.

(66) Sun, H.; Zeng, Y.; Pang, K. S. Interplay of Phase II Transporters and Enzymes in Futile Cycling: Influence of Estradiol 17β D-glucuronide and Estradiol 3-sulfate-17β-D glucuronide Excretion by Mrp2 on Net Sulfation in TR^- and Wistar Perfused Rat Liver Preparations. *Drug Metab. Dispos.*, under revision.

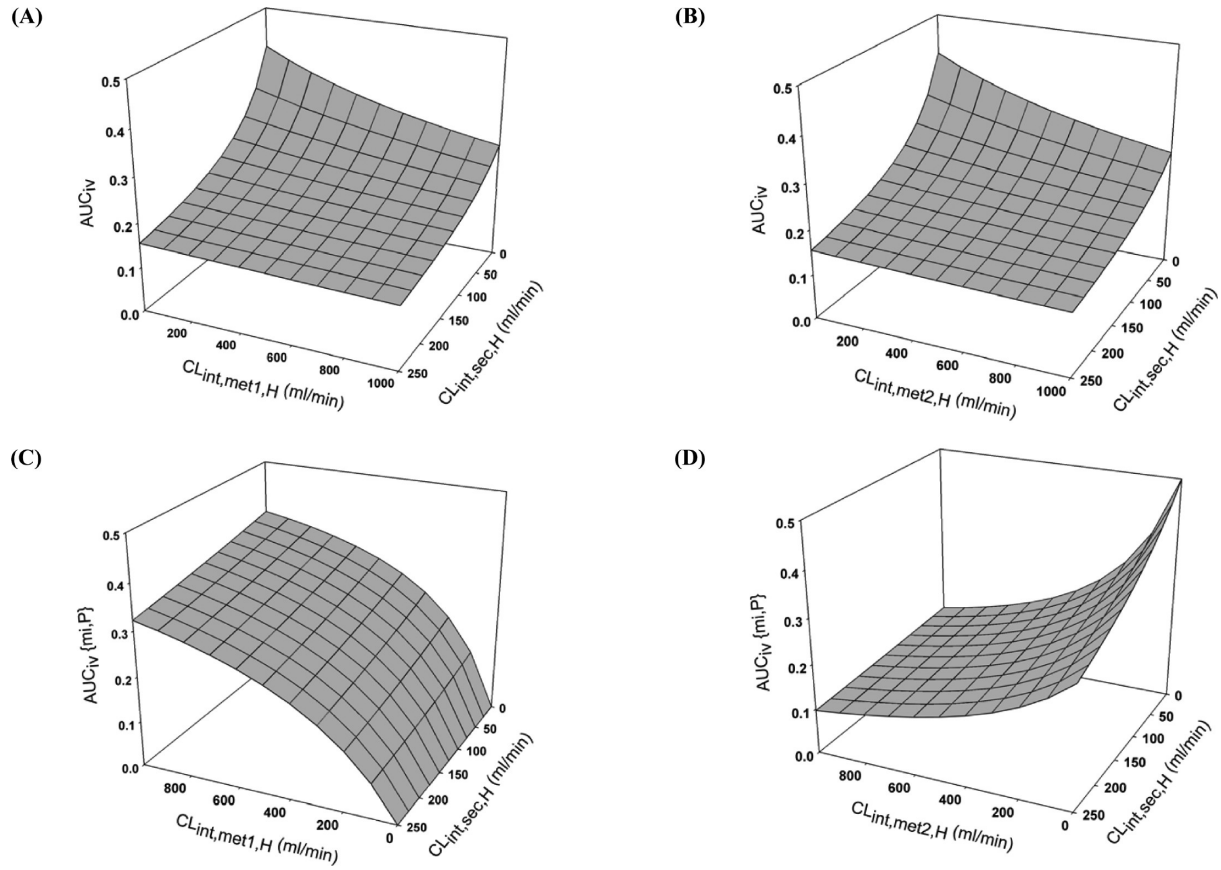

Figure 6. Simulated effects of $CL_{int,met1,H}$ and $CL_{int,sec,H}$ on the area under the curve (AUC) for parent drug and metabolite, AUC_{iv} and $AUC_{iv}\{mi,P\}$, respectively, after intravenous doses of 100 drug units. Q_H was set at 1,500 mL/min; $CL_{d1} = CL_{d2} = 6Q_H$; $CL_{in}^{H} = CL_{ef}^{H} = 1000$ mL/min. For (A) and (B), $CL_{int,met2,H} = 300$ mL/min, whereas for (C) and (D), $CL_{int,met1,H} = 300$ mL/min.

$AUC_L\{mi,P\}$ in the presence of futile cycling (Table 4). The area under the curve for the precursor in reservoir, AUC_R, is modulated by all the intrinsic clearances of the precursor, including basolateral influx (CL_{in}^{H}) and efflux (CL_{ef}^{H}), metabolic ($CL_{int,met}^{D\rightarrow Mi}$ and $CL_{int,met}^{other}$) and secretory ($CL_{int,sec,H}$) intrinsic clearances. The net metabolite formation intrinsic clearance of the precursor ($ef_m''\ CL_{int,met}^{D\rightarrow Mi}$) is reduced by the factor of ($1 - ef_m''$), or ($CL_{int,met}^{Mi\rightarrow D}\{mi\}$)/($CL_{int,sec,H}\{mi\} + CL_{int,met}^{Mi\rightarrow D}\{mi\} + CL_{int,met}^{other}\{mi\}$). The area under the curve for the formed metabolite in the reservoir, $AUC_R\{mi,P\}$, is modulated by parameters relating to metabolite handling ($CL_{in}^{H}\{mi\}$, $CL_{ef}^{H}\{mi\}$, $CL_{int,sec,H}\{mi\}$, $CL_{int,met}^{Mi\rightarrow D}\{mi\}$) and metabolite formation ($CL_{int,met}^{D\rightarrow Mi}$), and the intrinsic clearances for the handling of the parent drug: $CL_{int,sec,H}$, $CL_{int,met}^{other}$ and $CL_{int,met}^{D\rightarrow Mi}$. Analogously, the cumulative excretion of the precursor ($A_{e,\infty}$) and metabolite ($A_{e,\infty}\{mi,P\}$) are modified by ef_m'' or ef_m' when futile cycling exists. The apparent total (CL_H) and excretory ($CL_{H,ex}$) clearances of the liver may be estimated as dose/AUC_R and $A_{e,\infty}/AUC_R$, respectively, whereas the apparent metabolic clearance ($CL_{H,met}$) is obtained from the difference between CL_H and $CL_{H,ex}$ (Table 5). In the absence of a membrane barrier, the transmembrane clearances are very high: $CL_{in}^{H} = CL_{ef}^{H} \gg$ all of the intrinsic clearance terms, $CL_{int,sec,H}$, ($ef_m''\ CL_{int,met}^{D\rightarrow Mi}$) and $CL_{int,met}^{other}$. As noted, ef_m'', together with $CL_{int,met}^{D\rightarrow Mi}$, appears in the solutions of all the apparent clearances (Table 5). These solved relationships (Tables 4 and 5) allow the examination of transporter−enzyme interplay as described in the ensuing section.

Examples. Examples on transporter−enzyme interplay in the liver are numerous. Animal studies with P-gp of single (*mdr1a*(−/−)) or double (*mdr1a/1b*(−/−)) knockout mice showed higher AUCs and reduced clearance of [^{14}C]*N*-methyl erythromycin, vinblastine, paclitaxel, tacrolimus, digoxin, cyclosporin A, doxorubicin, abacavir, cetirizine, loratadine, desloratadine, hydroxyzine, diphenhydramine, triprolidine, glabridin, topotecan, and sulfasalazine *in vivo* when P-gp was absent (Table 6). The % dose of [^{14}C]*N*-methyl erythromycin that was converted to $^{14}CO_2$ as the product of Cyp3a metabolism was significantly increased, as revealed by the "erythromycin breath test", in *mdr1a/1b*(−/−) mice compared to *mdr1a/1b*(+/+) mice after an intravenous dose, despite a lack of change in the Cyp3a content.[76] In general, the absence of P-gp resulted in enhanced Cyp3a-mediated metabolism *in vivo*, as also predicted by Table 3. Chiou[84] and Jeong and Chiou[85] also observed that absence of P-gp resulted in an apparent reduction in the hepatic clearance of tacrolimus.

The competition between the Mrp2 and the Sult1e1, or estrogen sulfotransferase, was examined in the perfused liver with estradiol 17β D-glucuronide ($E_2$17G) and its sulfated

Table 4. Analytical Solutions for the AUC for the Parent Drug (AUC_R and AUC_L) and Formed Metabolite ($AUC_R\{mi,P\}$ and $AUC_L\{mi,P\}$) in Reservoir and Liver Tissue and Cumulative Amounts of Biliary Excretion of the Parent Drug ($A_{e,\infty}$) and Metabolite ($A_{e,\infty}\{mi,P\}$) for a Drug−Metabolite Pair (reproduced from reference 66, with permission)[a]

Terms	Solutions
AUC_R[b]	$\dfrac{Dose_{iv}\left[Q_H(CL_{ef}^H + CL_{int,sec,H} + ef_m'' CL_{int,met}^{D\to Mi} + CL_{int,met}^{other}) + f_B CL_{in}^H (CL_{int,sec,H} + ef_m'' CL_{int,met}^{D\to Mi} + CL_{int,met}^{other})\right]}{Q_H f_B CL_{in}^H (CL_{int,sec,H} + ef_m'' CL_{int,met}^{D\to Mi} + CL_{int,met}^{other})}$
$AUC_R\{mi,P\}$[c]	$\dfrac{Dose_{iv}\ CL_{ef}^H\{mi\} CL_{int,met}^{D\to Mi}}{f_B\{mi\}\ CL_{in}^H\{mi\}(CL_{int,sec,H} + CL_{int,met}^{D\to Mi} + CL_{int,met}^{other})(CL_{int,sec,H}\{mi\} + ef_m'\ CL_{int,met}^{Mi\to D}\{mi\} + CL_{int,met}^{other}\{mi\})}$
AUC_L	$\dfrac{Dose_{iv}}{f_L(CL_{int,sec,H} + CL_{int,met}^{other} + ef_m'' CL_{int,met}^{D\to Mi})}$
$AUC_L\{mi,P\}$	$\dfrac{Dose_{iv}\ CL_{int,met}^{D\to Mi}}{f_L\{mi\}(CL_{int,sec,H} + CL_{int,met}^{D\to Mi} + CL_{int,met}^{other})(CL_{int,sec,H}\{mi\} + ef_m' CL_{int,met}^{Mi\to D}\{mi\} + CL_{int,met}^{other}\{mi\})}$
$A_{e,\infty}$	$\dfrac{Dose_{iv}\ CL_{int,sec,H}}{(CL_{int,sec,H} + CL_{int,met}^{other} + ef_m'' CL_{int,met}^{D\to Mi})}$
$A_{e,\infty}\{mi,P\}$	$\dfrac{Dose_{iv} CL_{int,met}^{D\to Mi} CL_{int,sec,H}\{mi\}}{(CL_{int,sec,H} + CL_{int,met}^{D\to Mi} + CL_{int,met}^{other})(CL_{int,sec,H}\{mi\} + ef_m' CL_{int,met}^{Mi\to D}\{mi\} + CL_{int,met}^{other}\{mi\})}$

[a] in absence ($CL_{int,met}^{Mi\to D}\{mi\} = 0$) and presence ($CL_{int,met}^{Mi\to D}\{mi\} > 0$) of futile cycling

[b] ef_m'',effective coefficient for metabolite formation, $ef_m'' = \dfrac{CL_{int,sec,H}\{mi\} + CL_{int,met}^{other}\{mi\}}{CL_{int,sec,H}\{mi\} + CL_{int,met}^{Mi\to D}\{mi\} + CL_{int,met}^{other}\{mi\}}$.

In absence of futile cycling, $CL_{int,met}^{Mi\to D}\{mi\} = 0$, rendering $ef_m'' = 1$; in presence of futile cycling, $CL_{int,met}^{Mi\to D}\{mi\} > 0$, rendering $0 < ef_m'' < 1$.

[c] ef_m', effective recycling coefficient, $ef_m' = \dfrac{CL_{int,sec,H} + CL_{int,met}^{other}}{CL_{int,sec,H} + CL_{int,met}^{D\to Mi} + CL_{int,met}^{other}}$.

Table 5. Analytical Solutions for Metabolic ($CL_{H,met}$), Excretory ($CL_{H,ex}$), and Total Hepatic (CL_H) Clearances in the Presence of Futile Cycling (reproduced from reference 66, with permission)

Clearances[a]	With Barrier	Without Barrier ($CL_{in}^H = CL_{in}^H >> CL_{int,sec,H}$, $ef_m' CL_{int,met}^{D\to Mi}$ or $CL_{int,met}^{other}$)
$CL_{H,ex}$[b] (Biliary clearance)	$\dfrac{Q_H f_B CL_{in}^H CL_{int,sec,H}}{\left[Q_H(CL_{ef}^H + CL_{int,sec,H} + ef_m'' CL_{int,met}^{D\to Mi} + CL_{int,met}^{other}) + f_B CL_{in}^H (CL_{int,sec,H} + ef_m'' CL_{int,met}^{D\to Mi} + CL_{int,met}^{other})\right]}$	$\dfrac{Q_H f_B CL_{int,sec,H}}{\left[Q_H + f_B(CL_{int,sec,H} + ef_m'' CL_{int,met}^{D\to Mi} + CL_{int,met}^{other})\right]}$
$CL_{H,met}$ (Metabolic clearance)	$\dfrac{Q_H f_B CL_{in}^H (ef_m'' CL_{int,met}^{D\to Mi} + CL_{int,met}^{other})}{\left[Q_H(CL_{ef}^H + CL_{int,sec,H} + ef_m'' CL_{int,met}^{D\to Mi} + CL_{int,met}^{other}) + f_B CL_{in}^H (CL_{int,sec,H} + ef_m'' CL_{int,met}^{D\to Mi} + CL_{int,met}^{other})\right]}$	$\dfrac{Q_H f_B (ef_m'' CL_{int,met}^{D\to Mi} + CL_{int,met}^{other})}{\left[Q_H + f_B(CL_{int,sec,H} + ef_m'' CL_{int,met}^{D\to Mi} + CL_{int,met}^{other})\right]}$
CL_H (Total hepatic clearance)	$\dfrac{Q_H f_B CL_{in}^H (CL_{int,sec,H} + ef_m'' CL_{int,met}^{D\to Mi} + CL_{int,met}^{other})}{\left[Q_H(CL_{ef}^H + CL_{int,sec,H} + ef_m'' CL_{int,met}^{D\to Mi} + CL_{int,met}^{other}) + f_B CL_{in}^H (CL_{int,sec,H} + ef_m'' CL_{int,met}^{D\to Mi} + CL_{int,met}^{other})\right]}$	$\dfrac{Q_H f_B (CL_{int,sec,H} + ef_m'' CL_{int,met}^{D\to Mi} + CL_{int,met}^{other})}{\left[Q_H + f_B(CL_{int,sec,H} + ef_m'' CL_{int,met}^{D\to Mi} + CL_{int,met}^{other})\right]}$

[a] The solutions for CL_H and $CL_{H,ex}$ were obtained by $Dose/AUC_R$ and $A_{e,\infty}/AUC_R$, respectively. The metabolic clearance was estimated by the difference of CL_H and $CL_{H,ex}$.

[b] ef_m'', effective coefficient for metabolite formation, $ef_m'' = \dfrac{CL_{int,sec,H} + CL_{int,met}^{other}\{mi\}}{CL_{int,sec,H}\{mi\} + CL_{int,met}^{Mi\to D}\{mi\} + CL_{int,met}^{other}\{mi\}}$.

metabolite, estradiol 3-sulfate-17β-glucuronide, E_23S17G; both E_217G and E_23S17G were substrates of Mrp2.[65] E_217G is representative of a highly cleared drug in the rat liver whose entry is mediated by Oatp1a1, Oatp1a4, and Oatp1b2. Futile cycling, or the interconversion between a parent drug and metabolite, occurs between E_217G and E_23S17G to a modest extent since E_23S17G is desulfated back to E_217G by the arylsulfatase. The commensurate decrease in Oatp-

Table 6. Literature Data on AUC and CL after Intravenous Administrations to Wild Type and P-gp Single *mdr1a*(−/−) or Double *mdr1a/1b*(−/−) Knockout *mdr1a*(−/−) Mice

	AUC (ng/mL-h)		CL (L/h/kg)		
	wild type	*mdr1a*(−/−) or *mdr1a/1b*(−/−)	wild type	*mdr1a*(−/−) or *mdr1a/1b*(−/−)	ref
vinblastine (1 and 6 mg/kg)	99	157	10.1	6.4	67
	1015	1470	5.9	4.3	
paclitaxel (10 mg/kg)	4450	9100	2.24	1.10	68
FK506 (2 mg/kg)	563	1323	3.35	1.16	69
digoxin (1 mg/kg)	2590	7330	0.386	0.136	70
cyclosporin A (1 mg/kg)	1783	1984	0.558	0.504	71
doxorubicin (5 mg/kg)	1054	1316	4.5	3.6	72
tacrolimus (2 mg/kg)	598	1733	3.35	1.16	69
paclitaxel (10 mg/kg)	4783	5701	2.09	1.73	73
abacavir (10 mg/kg)	967	1817	10.3	5.46	74
cetirizine (5 mg/kg)	ND[a]	ND	0.45	0.324[b]	75
loratadine (5 mg/kg)	ND	ND	5.94	4.98[b]	75
desloratadine (5 mg/kg)	ND	ND	1.38	1.2[b]	75
hydroxyzine (5 mg/kg)	ND	ND	4.8	4.2[b]	75
diphenhydramine (5 mg/kg)	ND	ND	3.96	3.72[b]	75
triprolidine (5 mg/kg)	ND	ND	8.04	7.14[b]	75
[^{14}C]*N*-methyl erythromycin (10 μCi/kg)	22.2[c]	34.2/42.3[b,c]	ND	ND	76
glabridin (5 mg/kg)	82[d]	389[d]	ND	ND	77
tanshinone (5 mg/kg)	64[d]	656[d]	ND	ND	78
diastereomer pair of Alphavbeta3-Antagonists (5 mg/kg)	1.35[d]	2.99[d]	ND	ND	79
grepafloxacin (5 mg/kg)	ND	ND	2.97	2.05/2.35[b]	80
cyclosporin A (10 mg/kg)	40000	62000	0.248[b]	0.161[b]	81
topotecan (5 mg/kg)	475	352[b]	ND	ND	82
sulfasalazine (5 mg/kg)	5131	3504	0.87	0.47	83

[a] ND, not determined. [b] *mdr1a/1b* (−/−). [c] dose %/min. [d] Oral administration.

mediated transport during tumor metastasis in the Wag−Rij rat failed to alter the clearance of $E_2$17G, since the transport activity remained high.[65] The increase in Sult1e1 that also accompanied tumor development led to increased metabolic clearance, $CL_{H,met}$ and decreased the biliary clearance, $CL_{H,ex}$, despite that Mrp2 was unchanged; the total hepatic clearance, CL_H, remained basically flow-limited and unchanged.[65] These changes were in agreement with the predictions on the reciprocal relationship between enzyme and transporter.

The backward conversion of $E_2$3S17G to the parent drug $E_2$17G further adds complexity to transporter−enzyme interplay. Futile cycling empowers the metabolite, $E_2$3S17G, to exert considerable effects on the kinetics of parent drug. It is intuitive that, when excretion of the formed conjugate is curtailed, cellular concentrations of both the formed metabolite and parent drug would rise. Expectedly, transporters and enzymes for the handling of the metabolite should affect the kinetics and metabolism of the parent drug. When $E_2$17G and $E_2$3S17G were applied in recirculating liver perfusion studies to examine the interplay of phase II conjugation enzyme and transporter in Wistar (control) and the Mrp2-deficient TR$^-$ rats, a drastic reduction in the biliary secretion of $E_2$17G and $E_2$3S17G, dramatically higher liver concentrations of $E_2$17G and $E_2$3S17G, decreased net metabolism of $E_2$17G, and attainment of steady state for $E_2$17G and $E_2$3S17G in reservoir perfusate were observed for the TR$^-$ rats compared to that of the control Wistar rats.[66] These outcomes were predicted by the PBPK model, whose simulations further showed the important role of the Mrp2 (and $CL_{int,sec,H}$ and $CL_{int,sec,H}\{mi\}$) on AUCs in the reservoir and liver for $E_2$17G and $E_2$3S17G (Figure 7). Simulated profiles showed that the AUC's for both $E_2$17G and $E_2$3S17G increased gradually when the majority of Mrp2 activity was blunted (<80%), and when Mrp2 activity was almost totally blunted (>80%), the AUCs were elevated precipitously toward infinity (Figure 7A). Correspondingly, all of the liver clearances were decreased upon the reduction of Mrp2 activity and the values approached zero (Figure 7A). Other hypothetical simulations were conducted to mimic other scenarios in which the parent drug and the metabolite do not share the same canalicular transporter, when the secretory transporter activity toward the excretion of the metabolite (Figure 7B) or of the parent drug (Figure 7C) was reduced. The extents of change were not as dramatic as when both the precursor and metabolite secretory transporter activities were blunted (cf. Figures 7B and 7C vs Figure 7A). These changes were highly dependent on the backward conversion intrinsic clearance of the metabolite, another parameter that influences futile cycling.

Uptake and efflux transporters can modulate the rate of drug metabolism. Usually, studies are conducted with use

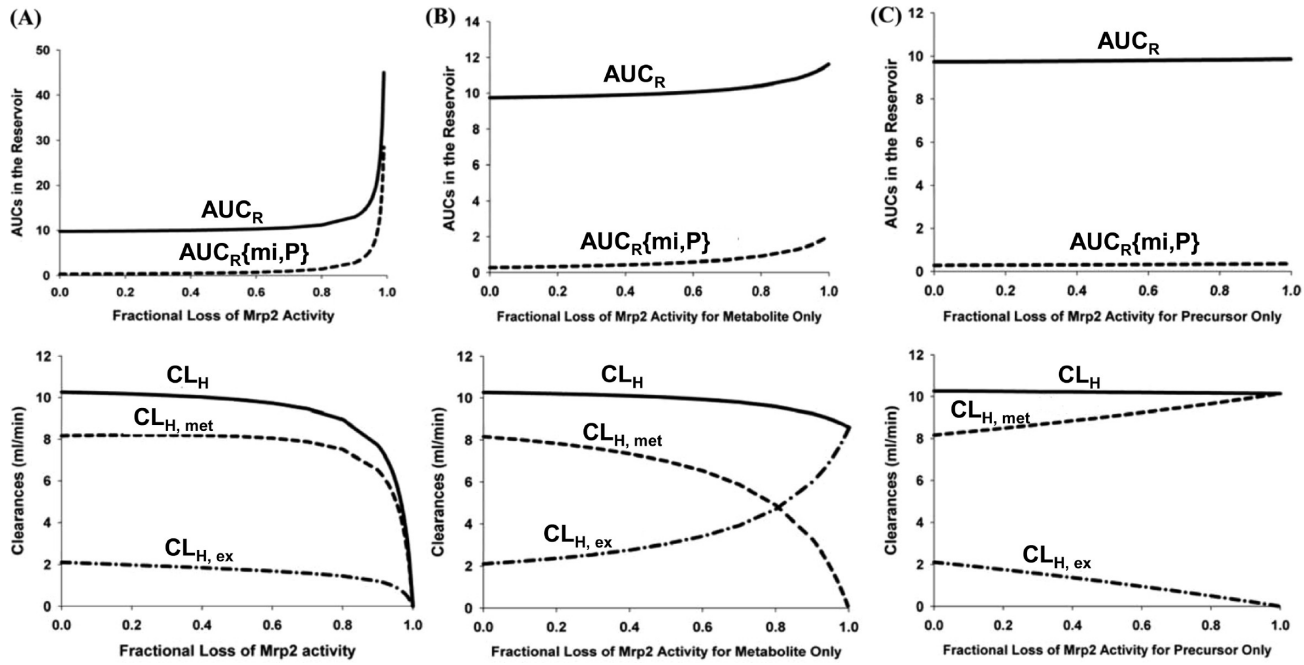

Figure 7. Futile cycling: interplay of phase II secretory excretion activity on net metabolism of the drug. Upper panel, simulated profiles for AUC_R (—) and $AUC_R\{mi,P\}$ (– –), and lower panel, the resultant metabolic (– –), excretory (– • –), and total (—) drug clearances upon reduction/loss of secretory activity, for (A) $CL_{int,sec,H}$ for the excretion of both parent drug and metabolite, (B) $CL_{int,sec,H}$ for the excretion of metabolite only, and (C) $CL_{int,sec,H}$ for the excretion of parent drug. The example was simulated based on perfusion data for Wistar and TR^- liver perfusion with $E_2$17G that undergoes futile cycling with its metabolite $E_2$3S17G, both of which are excreted by Mrp2 (reproduced from reference 66, with permission).

Table 7. Summary of Changes in Hepatic Clearances with Use of Inhibitors in Cell-Based, Perfusion, and *in Vivo* Systems[a]

Drug	Inhibitors	Observations	Deduction	References
Digoxin (10 μM) in hepatocytes	+ Rifampin 100 μM (Oatp) + GF120918 1 μM (P-gp)	↑AUC; ↓metabolite ↓AUC; ↑metabolite	• Rifampin inhibited CL_{in}^{H} for Oatp uptake (consistent) • GF120918 ↓ $CL_{H,ex}$ and promotes metabolism (consistent); • AUC was summed total of media+cell; poor parameter	88
Erythromycin (10 mg/kg) in hepatocytes and rat *in vivo*	+ Rifampin 2.5 mg/kg (Oatp) + GF120918 0.25 mg/kg (P-gp)	**Hepatocytes**: ↓ AUC_{cell}; and ↓ N-desmethyl metabolite by rifampin and ↑ AUC_{cell}; and ↑ N-desmethyl metabolite by GF120918 **In vivo**: ↑ AUC and ↑ metabolism for both rifampin and GF120918 ↓ CL_H; ↓ $CL_{H,ex}$	• **In hepatocyes**, rifampin inhibited erythromycin uptake and metabolism (consistent) whereas GF120918 inhibited erythromycin excretion and increased metabolism (consistent) • **In vivo:** rifampin and GF120918 decreased CL_H (consistent with reduced uptake and P-gp inhibition) • **In vivo:** ↑ metabolism with GF120918 (consistent with P-gp inhibition), but not for rifampin (not consistent with reduced uptake). The latter explanation was attributed to the N-desmethyl erythromycin metabolite being a substrate of both P-gp and Oatp and can compete for transport	89
Tacrolimus FK506 (100 μg) in perfused rat liver	+ Troleandomycin 20 μM (Cyp3a) + GF120918 1 μM (P-gp) + Cyclosporine 10 μM (Cyp3a & P-gp)	↑ AUC(30 min); ↑metabolite(30 min) ↓ AUC(30 min); ↓metabolite(30 min) ↑ AUC(30 min); ↑metabolite(30 min)	• ↓ CL_H (consistent); ↑ metabolism (inconsistent); poor AUC • ↑ CL_H (inconsistent); ↓ metabolism (inconsistent); poor AUC • ↓ CL_H (consistent); ↑ metabolism (consistent for P-gp inhibition but not for Cyp3a inhibition; greater P-gp inhibition)	90
Digoxin (10 μg) in perfused rat liver	+ Rifampin 100 μM (Oatp2) + Quinidine 10 μM (P-gp)	↑ AUC (60 min); ↓metabolite (60 min) ↓ AUC (60 min); ↑metabolite (60 min)	• ↓ CL_H (consistent); ↓ metabolism (consistent) • ↑ CL_H (inconsistent); ↑ metabolism (consistent with P-gp inhibition)	91
Atorvastatin or ATV (0.11 μmole) in perfused rat liver	+ Rifampin 5, 10, 50 μM (Oatp)	↑ AUC (60 min); ↑metabolite (60 min)	• ↓ CL_H (consistent); ↑metabolites (inconsistent); explained by 2-OH ATV and 4-OH ATV being substrates for Oatp1b2	92
Atorvastatin or ATV (2 mg/kg) in rat *in vivo*	+ Rifampin 20 mg/kg (Oatp)	↑ AUC ; ↑metabolite	• ↓ CL_H (consistent); ↑metabolites (inconsistent); explained by 2-OH ATV and 4-OH ATV being substrates for Oatp1b2	93
Digoxin (10 μg /kg) in rat *in vivo*	+ Amiodarone 20 mg/kg (Oatp2)	↑ AUC	• ↓ CL_H (consistent)	94
[^{14}C-*N*-methyl]Erythromycin (3 μCi) in human *in vivo*	+ Tariquidar 150 mg (P-gp)	↑ Erythromycin breath test (metabolite)	• ↑ metabolism (consistent)	95
Atorvastatin (40 mg) in human *in vivo*	+ Rifampin 600 mg (OATP)	↑ AUC; ↑metabolite	• ↓ CL_H (consistent); ↑metabolites (inconsistent); explained by 2-OH ATV and 4-OH ATV being substrates for OATP1B1	96
Atorvastatin (10 mg) in renal transplant recipients *in vivo*	+ Cyclosporine-based immunosuppressive therapy (CYP3A and OATP1B1)	↑ AUC; ↑metabolite	• ↓ CL_H (consistent); ↑metabolite (inconsistent), explained by ATV and metabolites being substrates for OATP1B1	97

[a] The deductions were made with the relations shown in Tables 2 and 3 and Figure 6.

of uptake or efflux transporter inhibitors. Table 7 summarizes recent studies with respect to the effect of inhibitors of hepatic uptake, efflux or metabolism on the hepatic metabolic, secretory, and total clearances. Tables 2 and 3 and Figure 6 were used to examine transporter−enzyme or enzyme−enzyme interplay in the liver, and how the changes

in the influx, efflux, metabolic, or secretory intrinsic clearances affect the metabolic, excretion, and total hepatic clearances. However, these relations mandate that the area under curve (AUC) of drug in the cell or media be fully characterized between time = 0 and time = ∞. This condition was not always satisfied, and the reported AUC estimate was often incomplete or poorly characterized. Sometimes, the AUC of drug in the media and cell were combined, and the AUC of drug in the cell or media was not reported.

In freshly prepared hepatocytes, P-gp can be internalized[64] and P-gp inhibition may render unexpectedly higher drug cellular levels when the drug is entrapped within vesicles; hence, the system may not be appropriate for the study of apical efflux transporter−enzyme interplay. Lam and Benet observed that rifampin, an inhibitor of Oatp1a4 transport, increased the total AUC of digoxin in hepatocytes and media whereas GF120918 reduced the AUC of digoxin.[86] The solved equations and trends in Tables 2 and 3 would not apply here, especially when the combined AUC of digoxin in media and the cell was reported. The total level of the Dg2 metabolite (found in combined cell and media) decreased in the presence of rifampin and rose with GF120918, trends expected for decreased influx and inhibited P-gp, respectively. Lam et al. also used rifampin and GF120918 to examine changes in erythromycin metabolism to the *N*-desmethyl erythromycin metabolite in freshly prepared isolated hepatocytes and the rat *in vivo*.[87] Separation of the cell and total (media + cell) was performed; reduced cellular accumulation of erythromycin and formation of the total *N*-desmethyl erythromycin metabolite was observed with rifampicin over controls.[87] Increased intracellular accumulation of erythromycin and increased formation of *N*-desmethyl erythromycin metabolite in both media and cell were observed with GF120918 versus the controls[87] (Table 7). These changes in intracellular erythromycin accumulation vs metabolism of erythromycin that accompanied rifampcin and GF120918 were predicted by Tables 2 and 3. With intravenous dosing *in vivo*, rifampin increased erythromycin AUC and reduced the total clearance of erythromycin, whereas GF120918 increased the AUC{mi,P};[87] these events (Table 7) were also predicted by Table 3.

(67) van Asperen, J.; Schinkel, A. H.; Beijnen, J. H.; Nooijen, W. J.; Borst, P.; van Tellingen, O. Altered Pharmacokinetics of Vinblastine in Mdr1a P-Glycoprotein-Deficient Mice. *J. Natl. Cancer Inst.* **1996**, *88*, 994–999.

(68) Sparreboom, A.; van Asperen, J.; Mayer, U.; Schinkel, A. H.; Smit, J. W.; Meijer, D. K.; Borst, P.; Nooijen, W. J.; Beijnen, J. H.; van Tellingen, O. Limited Oral Bioavailability and Active Epithelial Excretion of Paclitaxel (Taxol) Caused by P-Glycoprotein in the Intestine. *Proc. Natl. Acad. Sci. U.S.A.* **1997**, *94*, 2031–2035.

(69) Yokogawa, K.; Takahashi, M.; Tamai, I.; Konishi, H.; Nomura, M.; Moritani, S.; Miyamoto, K.; Tsuji, A. P-Glycoprotein-Dependent Disposition Kinetics of Tacrolimus: Studies in Mdr1a Knockout Mice. *Pharm. Res.* **1999**, *16*, 1213–1218.

(70) Kawahara, M.; Sakata, A.; Miyashita, T.; Tamai, I.; Tsuji, A. Physiologically Based Pharmacokinetics of Digoxin in Mdr1a Knockout Mice. *J. Pharm. Sci.* **1999**, *88*, 1281–1287.

(71) Kwei, G. Y.; Alvaro, R. F.; Chen, Q.; Jenkins, H. J.; Hop, C. E.; Keohane, C. A.; Ly, V. T.; Strauss, J. R.; Wang, R. W.; Wang, Z.; Pippert, T. R.; Umbenhauer, D. R. Disposition of Ivermectin and Cyclosporin A in CF-1 Mice Deficient in Mdr1a P-Glycoprotein. *Drug Metab. Dispos.* **1999**, *27*, 581–587.

(72) van Asperen, J.; van Tellingen, O.; Tijssen, F.; Schinkel, A. H.; Beijnen, J. H. Increased Accumulation of Doxorubicin and Doxorubicinol in Cardiac Tissue of Mice Lacking Mdr1a P-Glycoprotein. *Br. J. Cancer* **1999**, *79*, 108–113.

(73) Bardelmeijer, H. A.; Beijnen, J. H.; Brouwer, K. R.; Rosing, H.; Nooijen, W. J.; Schellens, J. H.; van Tellingen, O. Increased Oral Bioavailability of Paclitaxel by GF120918 in Mice through Selective Modulation of P-Glycoprotein. *Clin. Cancer Res.* **2000**, *6*, 4416–4421.

(74) Shaik, N.; Giri, N.; Pan, G.; Elmquist, W. F. P-Glycoprotein-Mediated Active Efflux of the Anti-HIV1 Nucleoside Abacavir Limits Cellular Accumulation and Brain Distribution. *Drug Metab. Dispos.* **2007**, *35*, 2076–2085.

(75) Chen, C.; Hanson, E.; Watson, J. W.; Lee, J. S. P-Glycoprotein Limits the Brain Penetration of Nonsedating but Not Sedating H1-Antagonists. *Drug Metab. Dispos.* **2003**, *31*, 312–318.

(76) Lan, L. B.; Dalton, J. T.; Schuetz, E. G. Mdr1 Limits Cyp3A Metabolism in Vivo. *Mol. Pharmacol.* **2000**, *58*, 863–869.

(77) Cao, J.; Chen, X.; Liang, J.; Yu, X. Q.; Xu, A. L.; Chan, E.; Wei, D.; Huang, M.; Wen, J. Y.; Yu, X. Y.; Li, X. T.; Sheu, F. S.; Zhou, S. F. Role of P-Glycoprotein in the Intestinal Absorption of Glabridin, an Active Flavonoid from the Root of Glycyrrhiza Glabra. *Drug Metab. Dispos.* **2007**, *35*, 539–553.

(78) Yu, X. Y.; Lin, S. G.; Zhou, Z. W.; Chen, X.; Liang, J.; Liu, P. Q.; Duan, W.; Chowbay, B.; Wen, J. Y.; Li, C. G.; Zhou, S. F. Role of P-Glycoprotein in the Intestinal Absorption of Tanshinone Iia, a Major Active Ingredient in the Root of Salvia Miltiorrhiza Bunge. *Curr. Drug Metab.* **2007**, *8*, 325–340.

(79) Prueksaritanont, T.; Meng, Y.; Ma, B.; Leppert, P.; Hochman, J.; Tang, C.; Perkins, J.; Zrada, M.; Meissner, R.; Duggan, M. E.; Lin, J. H. Differences in the Absorption, Metabolism and Biliary Excretion of a Diastereomeric Pair of Alphavbeta3-Antagonists in Rat: Limited Role of P-Glycoprotein. *Xenobiotica* **2002**, *32*, 207–220.

(80) Sasabe, H.; Kato, Y.; Suzuki, T.; Itose, M.; Miyamoto, G.; Sugiyama, Y. Differential Involvement of Multidrug Resistance-Associated Protein 1 and P-Glycoprotein in Tissue Distribution and Excretion of Grepafloxacin in Mice. *J. Pharmacol. Exp. Ther.* **2004**, *310*, 648–655.

(81) Jin, M.; Shimada, T.; Yokogawa, K.; Nomura, M.; Ishizaki, J.; Piao, Y.; Kato, Y.; Tsuji, A.; Miyamoto, K. Site-Dependent Contributions of P-Glycoprotein and Cyp3A to Cyclosporin A Absorption, and Effect of Dexamethasone in Small Intestine of Mice. *Biochem. Pharmacol.* **2006**, *72*, 1042–1050.

(82) de Vries, N. A.; Zhao, J.; Kroon, E.; Buckle, T.; Beijnen, J. H.; van Tellingen, O. P-Glycoprotein and Breast Cancer Resistance Protein: Two Dominant Transporters Working Together in Limiting the Brain Penetration of Topotecan. *Clin. Cancer Res.* **2007**, *13*, 6440–6449.

(83) Zaher, H.; Khan, A. A.; Palandra, J.; Brayman, T. G.; Yu, L.; Ware, J. A. Breast Cancer Resistance Protein (Bcrp/Abcg2) Is a Major Determinant of Sulfasalazine Absorption and Elimination in the Mouse. *Mol. Pharmaceutics* **2006**, *3*, 55–61.

(84) Chiou, W. L.; Chung, S. M.; Wu, T. C. Potential Role of P-Glycoprotein in Affecting Hepatic Metabolism of Drugs. *Pharm. Res.* **2000**, *17*, 903–905.

(85) Jeong, H.; Chiou, W. L. Role of P-Glycoprotein in the Hepatic Metabolism of Tacrolimus. *Xenobiotica* **2006**, *36*, 1–13.

The hypothesis that apical efflux increased the metabolism was tested with tacrolimus, a substrate of both Cyp3a and P-gp, in the recirculating perfused liver preparation with GF120918 (P-gp inhibitor), troleandomycin (Cyp3a inhibitor), and cyclosporine (Cyp3a and P-gp inhibitor).[88] However, the chosen inhibitor often exhibits multiple inhibitory activities toward the basolateral influx/efflux transporters, Cyp3a, and P-gp, as suggested for cyclosporine.[95] The AUC of tacrolimus was increased by troleandomycin and cyclosporin coadministration, as expected of inhibition of either metabolism and/or excretion. The unexpected, lower AUC of tacrolimus observed with GF120918 was attributed by the authors as a greater exposure of tacrolimus to the enzyme, increasing the metabolic clearance (lower AUC) because of inhibited canalicular transport.[88] The lower AUC that translates to a higher total hepatic clearance is incongruent with the solved equations and trends shown in Tables 2 and 3. According to the pharmacokinetic analyses, the metabolic clearance should increase and total clearance, decrease, with inhibition of P-gp, rendering a higher and not lower AUC (see Table 2). The unexpected lower tacrolimus AUC[88] might have been due to inhibition of efflux. In other recirculating liver perfusion studies, digoxin displayed increased AUC and decreased formation of metabolites in the presence of rifampin for Oatp inhibition, as expected from Table 3, and decreased AUC of digoxin and increased metabolite formation with quinidine for P-gp inhibition.[89] Although reduced apical efflux was expected to bring about increased metabolism, the lower AUC of digoxin, implying an increase in total clearance, could not be readily explained (see Table 3) unless digoxin efflux was inhibited. In other studies, rifampin led to increased AUCs of atorvastatin and its hydroxylated metabolites in the perfused rat liver preparation, observations that were explained by inhibition of the uptake of both parent drug and metabolite species being substrates of Oatp (Table 7).[90]

VI. Transporter−Enzyme Interplay in the Intestine

The majority of oral drug absorption takes place at the small intestine and not the stomach because of the abundance of villi and microvilli that dramatically increase the surface area for passive diffusion. The drug, whether a weak acid or weak base, exhibits different extents of ionization at the pHs for stomach (1.3) and intestine (6) along the gastrointestinal tract, and drugs of higher lipophilicity exhibit a greater membrane permeation than the ionic counterparts. The absorptive and efflux transporters are found to coexist within enterocytes at the villus tip, and enzymes and transporters again compete for the drug within the cell.

Transporter−enzyme interplay is a common occurrence in the small intestine. The P450s and P-gp are important proteins in the small intestine, as in the liver, that delimit the absorption of drugs.[96−101] The controversy that exists for the Caco-2 monolayer also exists for the small intestine. Generally speaking, CYP3A4-meditated metabolism and P-gp-meditated efflux exert complementary roles in reducing the absorption of a drug and possibly its metabolites across enterocytes. The crucial effects of inhibition of P-gp on parent drug metabolism and transporter−enzyme interplay are based on the same fundamentals: namely, intestinal drug metabolism and excretion are influenced directly by the level of drug within the enterocytes, which is governed by the degree of P-gp-mediated efflux and metabolism, and drug permeability (entry and efflux) into the enterocyte. While some camps assert the view that increased secretion enhances metabolism due to prolongation of MRT,[33] Pang and colleagues hold the opinion that enhanced metabolism occurs when secretion is reduced (and not increased), and reduced metabolism occurs when secretion is increased.[98,102] The competing pathway will result in perturbation of the drug concentration in the intestinal cell and alter the relative rates.

(86) Lam, J. L.; Benet, L. Z. Hepatic Microsome Studies Are Insufficient to Characterize in Vivo Hepatic Metabolic Clearance and Metabolic Drug-Drug Interactions: Studies of Digoxin Metabolism in Primary Rat Hepatocytes Versus Microsomes. *Drug Metab. Dispos.* **2004**, *32*, 1311–1316.

(87) Lam, J. L.; Okochi, H.; Huang, Y.; Benet, L. Z. In Vitro and in Vivo Correlation of Hepatic Transporter Effects on Erythromycin Metabolism: Characterizing the Importance of Transporter-Enzyme Interplay. *Drug Metab. Dispos.* **2006**, *34*, 1336–1344.

(88) Wu, C. Y.; Benet, L. Z. Disposition of Tacrolimus in Isolated Perfused Rat Liver: Influence of Troleandomycin, Cyclosporine, and GG918. *Drug Metab. Dispos.* **2003**, *31*, 1292–1295.

(89) Lau, Y. Y.; Wu, C. Y.; Okochi, H.; Benet, L. Z. Ex Situ Inhibition of Hepatic Uptake and Efflux Significantly Changes Metabolism: Hepatic Enzyme-Transporter Interplay. *J. Pharmacol. Exp. Ther.* **2004**, *308*, 1040–1045.

(90) Lau, Y. Y.; Okochi, H.; Huang, Y.; Benet, L. Z. Pharmacokinetics of Atorvastatin and Its Hydroxy Metabolites in Rats and the Effects of Concomitant Rifampicin Single Doses: Relevance of First-Pass Effect From Hepatic Uptake Transporters, and Intestinal and Hepatic Metabolism. *Drug Metab. Dispos.* **2006**, *34*, 1175–1181.

(91) Lau, Y. Y.; Okochi, H.; Huang, Y.; Benet, L. Z. Multiple Transporters Affect the Disposition of Atorvastatin and Its Two Active Hydroxy Metabolites: Application of in Vitro and Ex Situ Systems. *J. Pharmacol. Exp. Ther.* **2006**, *316*, 762–771.

(92) Funakoshi, S.; Murakami, T.; Yumoto, R.; Kiribayashi, Y.; Takano, M. Role of Organic Anion Transporting Polypeptide 2 in Pharmacokinetics of Digoxin and Beta-Methyldigoxin in Rats. *J. Pharm. Sci.* **2005**, *94*, 1196–1203.

(93) Kurnik, D.; Wood, A. J.; Wilkinson, G. R. The Erythromycin Breath Test Reflects P-Glycoprotein Function Independently of Cytochrome P450 3A Activity. *Clin. Pharmacol. Ther.* **2006**, *80*, 228–234.

(94) Lau, Y. Y.; Huang, Y.; Frassetto, L.; Benet, L. Z. Effect of OATP1B Transporter Inhibition on the Pharmacokinetics of Atorvastatin in Healthy Volunteers. *Clin. Pharmacol. Ther.* **2007**, *81*, 194–204.

(95) Hermann, M.; Asberg, A.; Christensen, H.; Holdaas, H.; Hartmann, A.; Reubsaet, J. L. Substantially Elevated Levels of Atorvastatin and Metabolites in Cyclosporine-Treated Renal Transplant Recipients. *Clin. Pharmacol. Ther.* **2004**, *76*, 388–391.

(96) Suzuki, H.; Sugiyama, Y. Role of Metabolic Enzymes and Efflux Transporters in the Absorption of Drugs from the Small Intestine. *Eur. J. Pharm. Sci.* **2000**, *12*, 3–12.

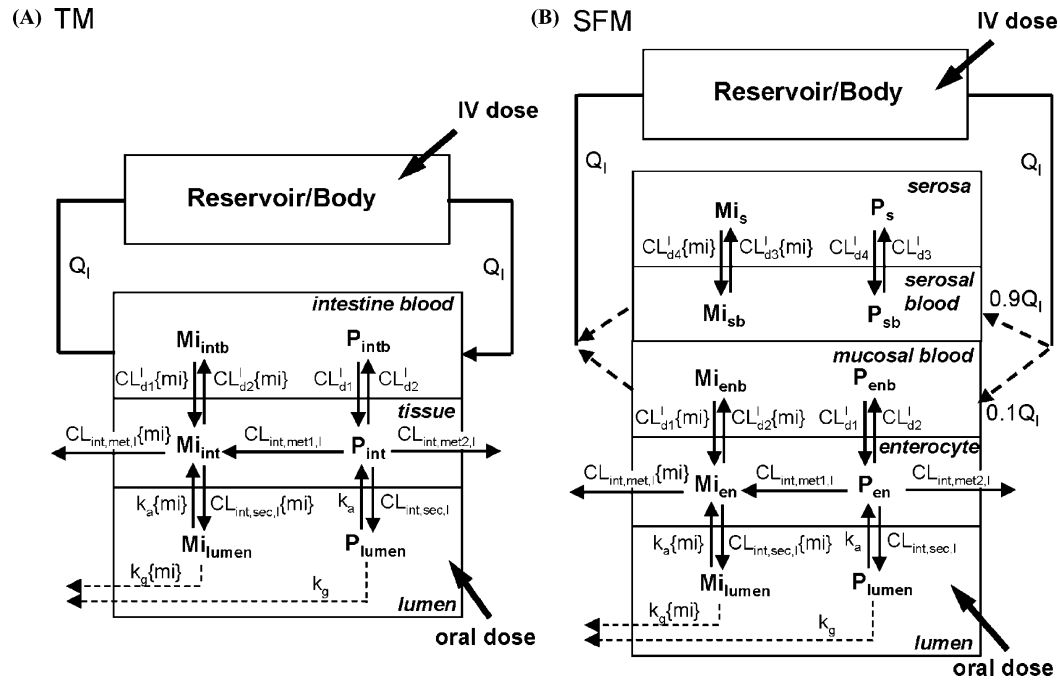

Figure 8. Physiologically based pharmacokinetic (PBPK) intestine models, the traditional model (TM) and the segregated flow model (SFM), with the intestine as the only elimination tissue. For TM, the intestinal blood (Q_l) perfuses the entire intestinal tissue, the site of metabolism and absorption from the lumen. For SFM, intestinal blood is segregated to perfuse the nonmetabolizing ($0.9Q_l$) and enterocyte-mucosal ($0.1Q_l$) regions. Drug equilibrates with those in the corresponding tissue layers with intrinsic transfer clearances CL^l_{d1} and CL^l_{d2} for TM, or CL^l_{d1} and CL^l_{d2}, CL^l_{d3} and CL^l_{d4} for SFM. The absorptive, metabolic, and efflux activities within the villus tips of the mucosal layer are represented by the rate constant, k_a, and metabolic and secretory intrinsic clearances, $CL_{int,met,l}$ and $CL_{int,sec,l}$, respectively; k_g is the rate constant that represents the loss in lumen either due to degradation or due to ineffective absorption (modified from ref 104 with permission).

Again, the reciprocal relationship between intestinal metabolism and excretion exists here for transporter−enzyme interplay.

PBPK Modeling of the Small Intestine: Traditional Model (TM) and Segregated Flow Model (SFM). A limited number of pharmacokinetic models have examined the influence of efflux and metabolism on oral drug absorption. Ito et al. employed a single "lumped" intestinal compartment model to investigate the influence of P-gp and CYP3A on intestinal drug absorption.[103] The results showed that the fraction absorbed after oral administration was increased following the inhibition of P-gp. Although this model accounted for the effect of drug metabolism, secretion and intracellular diffusion on drug absorption, the lack of consideration of intestinal blood flow allocation to different regions in intestine possibly renders this model unable to predict patterns of intestinal metabolism. Additionally, this model is not able to predict the effect of secretion on the metabolite formation.

Doherty and Pang used a traditional physiologically based pharmacokinetic model (TM) based on the intestine being a single homogeneous compartment to describe processes of intestinal absorption, metabolism, and secretion simultaneously, with all of the intestinal blood perfusing the tissue to account for oral drug bioavailability (Figure 8).[104] Due to the failure of the TM to predict route-dependent intestinal metabolism, which describes little or

(97) Wacher, V. J.; Salphati, L.; Benet, L. Z. Active Secretion and Enterocytic Drug Metabolism Barriers to Drug Absorption. *Adv. Drug Delivery Rev.* **2001**, *46*, 89–102.
(98) Pang, K. S. Modeling of Intestinal Drug Absorption: Roles of Transporters and Metabolic Enzymes (for the Gillette Review Series). *Drug Metab. Dispos.* **2003**, *31*, 1507–1519.
(99) Kivisto, K. T.; Niemi, M.; Fromm, M. F. Functional Interaction of Intestinal Cyp3A4 and P-Glycoprotein. *Fundam. Clin. Pharmacol.* **2004**, *18*, 621–626.
(100) von Richter, O.; Burk, O.; Fromm, M. F.; Thon, K. P.; Eichelbaum, M.; Kivisto, K. T. Cytochrome P450 3A4 and P-Glycoprotein Expression in Human Small Intestinal Enterocytes and Hepatocytes: A Comparative Analysis in Paired Tissue Specimens. *Clin Pharmacol. Ther.* **2004**, *75*, 172–183.
(101) Christians, U. Transport Proteins and Intestinal Metabolism: P-Glycoprotein and Cytochrome P4503A. *Ther. Drug Monit.* **2004**, *26*, 104–106.
(102) Cong, D.; Doherty, M.; Pang, K. S. A New Physiologically Based, Segregated-Flow Model to Explain Route-Dependent Intestinal Metabolism. *Drug Metab. Dispos.* **2000**, *28*, 224–235.
(103) Ito, K.; Kusuhara, H.; Sugiyama, Y. Effects of Intestinal Cyp3A4 and P-Glycoprotein on Oral Drug Absorption - Theoretical Approach. *Pharm. Res.* **1999**, *16*, 225–231.
(104) Doherty, M. M.; Pang, K. S. Route-Dependent Metabolism of Morphine in the Vascularly Perfused Rat Small Intestine Preparation. *Pharm. Res.* **2000**, *17*, 291–298.

Table 8. Solutions for AUC_{iv}, AUC_{po}, $AUC_{iv}\{mi\}$ and $AUC_{po}\{mi\}$ for the TM and SFM, with Intestine as the Only Eliminating Organ (from Ref 31 with Permission)

AUC terms	Solutions for the TM and SFM model
$AUC_{po}^{TM\ \&SFM}$	$\frac{F_{abs}Dose_{po}CL_{d2}^{I}}{CL_{d1}^{I}\left[\left(1-F_{abs}\right)CL_{int,sec,I}+CL_{int,met1,I}+CL_{int,met2,I}\right]}$
AUC_{iv}^{TM}	$\frac{Dose_{iv}\left[CL_{d1}^{I}\left[(1-F_{abs})CL_{int,sec,I}+CL_{int,met,I}\right]+Q_{I}\left[(1-F_{abs})CL_{int,sec,I}+CL_{int,met,I}+CL_{d1}^{I}\right]\right]}{Q_{I}CL_{d1}^{I}\left[(1-F_{abs})CL_{int,sec,I}+CL_{int,met,I}+CL_{int,met2,I}\right]}$
AUC_{iv}^{SFM}	$\frac{Dose_{iv}\left[CL_{d1}^{I}\left[(1-F_{abs})CL_{int,sec,I}+CL_{int,met,I}\right]+Q_{en}\left[(1-F_{abs})CL_{int,sec,I}+CL_{int,met,I}+CL_{d1}^{I}\right]\right]}{Q_{en}CL_{d1}^{I}\left[(1-F_{abs})CL_{int,sec,I}+CL_{int,met,I}+CL_{int,met2,I}\right]}$
$AUC_{po}\{mi,P\}^{TM\ \&SFM}$	$\frac{Dose_{po}F_{abs}CL_{int,met1,I}CL_{d2}^{I}\{mi\}}{\left[(1-F_{abs})CL_{int,sec,I}+CL_{int,met1,I}+CL_{int,met2,I}\right]CL_{d1}^{I}\{mi\}\left[\left(1-F_{abs}\{mi\}\right)CL_{int,sec,I}\{mi\}+CL_{int,met,I}\{mi\}\right]}$
$AUC_{iv}\{mi,P\}^{TM\ \&SFM}$	$\frac{Dose_{iv}CL_{int,met1,I}CL_{d2}^{I}\{mi\}}{\left[(1-F_{abs})CL_{int,sec,I}+CL_{int,met1,I}+CL_{int,met2,I}\right]CL_{d1}^{I}\{mi\}\left[\left(1-F_{abs}\{mi\}\right)CL_{int,sec,I}\{mi\}+CL_{int,met,I}\{mi\}\right]}$

no metabolism occurring after systemic dosing but notable metabolism existing following oral dosing, the segregated flow model (SFM) was developed to fill the gap.[102] This model describes that the majority of the intestinal blood flow perfuses the nonabsorptive and nonmetabolizing serosal and submucosal regions and only a low, partial flow perfuses the absorptive and metabolizing enterocyte region where the metabolic enzymes and the transporters are located (Figure 8). In order to explain the observed route-dependent intestinal metabolism of drugs, a similar strategy was used by the Simcyp group to describe intestinal drug clearance.[105] The intestine is not a closed system like the Caco-2 cells due to the possibility of irreversible loss described by the k_g. The f_{met} simulated for the TM and SFM following both intravenous and oral dosing displayed decreasing trends with increased apical secretory intrinsic clearances under first-order conditions. The MRT, however, may actually be decreased when $k_g > 0$ and is comparable to or greater than k_a for both TM or SFM (unpublished simulations of Eric Tseng and K. S. Pang). The reasoning that higher MRT resulted with higher $CL_{int,sec}$ to bring about increased metabolism is therefore invalid.

Utilizing these two models, Sun and Pang solved the AUC terms for parent drug and metabolite (Table 8).[31] The solutions for the TM and SFM for AUC_{po}, $AUC_{po}\{mi\}$ and $AUC_{iv}\{mi\}$ are found to be identical, whereas for the AUC_{iv}, the solution is similar except that Q_I exists for the solution for the TM and Q_{en} for the SFM. Simulations of the impact of varying k_a values on the AUC, shown by Sun and Pang, described that the secretory intrinsic clearance ($CL_{int,sec,I}$) is associated with the term $(1 - F_{abs})$, where F_{abs} is the fraction absorbed or $k_a/(k_a + k_g)$.[31] When the absorbed fraction, F_{abs}, is high ($\sim$1) due to the high k_a relative to k_g, net secretion is reduced to zero. The solutions agree with the hypothesis of Lin et al.,[106] who suggested that the role of P-gp on drug removal by the intestine is overemphasized. The $AUC_{po}\{mi\}$ and $AUC_{iv}\{mi\}$ are inversely related to the sum of $(1 - F_{abs})CL_{int,sec,I}$ and $CL_{int,met,I}$ (where $CL_{int,met,I} = CL_{int,met1,I} + CL_{int,met2,I}$). As $CL_{int,sec,I}$ increases, $AUC_{po}\{mi\}$ or $AUC_{iv}\{mi\}$ decreases; and, as $CL_{int,sec}$ decreases, $AUC_{po}\{mi\}$ or $AUC_{iv}\{mi\}$ increases. Due to the effective modulation of absorption on $CL_{int,sec,I}$ by F_{abs}, it appears that changes in $CL_{int,met,I}$ would exert a greater effect on drug bioavailability compared to similar changes in $CL_{int,sec,I}$. Moreover, when $CL_{int,sec,I}$ or $CL_{int,met,I}$ is increased (or decreased), the total clearance increased (or decreased) in unison. Based on the equations for the clearances, we summarize the expected effect of changes in influx, efflux, metabolic, secretion intrinsic clearances and rate constants on the apparent metabolic, excretion and total clearance in the intestine (Table 9).

Distributed Intestinal Models: The CAT, ACAT, Segmental Traditional and Segmental Segregated Flow Models. Since traditional models have treated the entire gastrointestinal tract as a single compartment, limitations exist since it is well recognized that the small intestine consists of three segmental regions of varying surface area, enzymes and transporters.[98] It was accepted that multiple compartments would better evaluate drug absorption and metabolism within the three segmental regions of the small

(105) Yang, J.; Jamei, M.; Yeo, K. R.; Rostami-Hodjegan, A. Prediction of intestinal first-pass drug metabolism. *Curr. Drug Metab.* **2007**, *8* (7), 676–684.

(106) Lin, J. H.; Chiba, M.; Baillie, T. A. Is the Role of the Small Intestine in First-Pass Metabolism Overemphasized. *Pharmacol. Rev.* **1999**, *51*, 135–158.

Table 9. General Trends of the Metabolic, Excretion, and Total Intestine Clearances When the Influx, Efflux, Metabolic, Secretory Intrinsic Clearances or Rate Constant Are Changed under Linear Conditions for the Intestine PBPK (TM or SFM) Models

	Intestinal Metabolic Clearance for formation of Mi_I $CL_{I,met1}$	Intestinal Metabolic Clearance for formation of other metabolites $CL_{I,met2}$	Intestinal Excretory $CL_{I,ex}$	Total Intestinal Clearance CL_I
$\uparrow CL^I_{d1}$ $\downarrow CL^I_{d2}$	↑	↑	↑	↑
$\downarrow CL^I_{d1}$ $\uparrow CL^I_{d2}$	↓	↓	↓	↓
$\uparrow CL_{int,met1,I}$ $\downarrow CL_{int,met1,I}$	↑ ↓	↓ ↑	↓ ↑	↑ ↓
$\uparrow CL_{int,met2,I}$ $\downarrow CL_{int,met2,I}$	↓ ↑	↑ ↓	↓ ↑	↑ ↓
$\uparrow CL_{int,sec,I}$ $\downarrow CL_{int,sec,I}$	↓ ↑	↓ ↑	↑ ↓	↑ ↓
$\uparrow k_a$ or $\downarrow (1\text{-}F_{abs})$ $\downarrow k_a$ or $\uparrow (1\text{-}F_{abs})$	↑ ↓	↑ ↓	↓ ↑	↓ ↑
$\uparrow k_g$ or $\uparrow (1\text{-}F_{abs})$ $\downarrow k_g$ or $\downarrow (1\text{-}F_{abs})$	↓ ↑	↓ ↑	↑ ↓	↑ ↓

intestine. Yu et al. developed a compartmental absorption and transit (CAT) model to account for the passive absorption, saturable absorption, degradation, and transit kinetics in the stomach and intestine and the transit flow in the human small intestine by considering the intestine as seven compartments.[107,108] The model is able to estimate the fraction of dose absorbed and the rate of drug absorption for passively transported drugs. Although the CAT model shows advantages of being able to predict the rate of drug absorption, there was the lack of consideration of drug metabolism and secretion. Another multiple compartmental absorption model that was developed by Shono and Willmann also contained the same limitation as the CAT model, though this model was able to account spatially for the varying pH values, length, radius, and effective surface area and drug dissolution kinetics, solubility and postabsorptive disposition parameters among different segments of the intestine.[109−111]

Pang and colleagues[98,112] extended the TM and SFM to segmental counterparts to account for differences in enzymes and transporters that exist along the length of the small intestine:[2,113−121] the segmental traditional model (STM) and the segmental segregated flow model (SSFM) (Figure 9). The results are two physiologically based, pharmacokinetic (PBPK) models of the small intestine that incorporate distributions of metabolic enzyme and efflux transporter along the length of the intestine to reflect segmental differences in enzymes and transporters.[98,112] Again, the STM views that the segmental flow (based on proportional

(107) Yu, L. X.; Amidon, G. L. Saturable Small Intestinal Drug Absorption in Humans: Modeling and Interpretation of Cefatrizine Data. *Eur. J. Pharm. Biopharm.* **1998**, *45*, 199–203.

(108) Yu, L. X.; Amidon, G. L. A Compartmental Absorption and Transit Model for Estimating Oral Drug Absorption. *Int. J. Pharm.* **1999**, *186*, 119–125.

(109) Shono, Y.; Jantratid, E.; Janssen, N.; Kesisoglou, F.; Mao, Y.; Vertzoni, M.; Reppas, C.; Dressman, J. B. Prediction of Food Effects on the Absorption of Celecoxib Based on Biorelevant Dissolution Testing Coupled with Physiologically Based Pharmacokinetic Modeling. *Eur. J. Pharm. Biopharm.* **2009**, *73*, 107–114.

(110) Willmann, S.; Edginton, A. N.; Dressman, J. B. Development and Validation of a Physiology-Based Model for the Prediction of Oral Absorption in Monkeys. *Pharm. Res.* **2007**, *24*, 1275–1282.

(111) Willmann, S.; Schmitt, W.; Keldenich, J.; Dressman, J. B. A Physiologic Model for Simulating Gastrointestinal Flow and Drug Absorption in Rats. *Pharm. Res.* **2003**, *20*, 1766–1771.

(112) Tam, D.; Tirona, R. G.; Pang, K. S. Segmental Intestinal Transporters and Metabolic Enzymes on Intestinal Drug Absorption. *Drug Metab. Dispos.* **2003**, *31*, 373–383.

(113) Paine, M. F.; Khalighi, M.; Fisher, J. M.; Shen, D. D.; Kunze, K. L.; Marsh, C. L.; Perkins, J. D.; Thummel, K. E. Characterization of Interintestinal and Intraintestinal Variations in Human Cyp3A-Dependent Metabolism. *J. Pharmacol. Exp. Ther.* **1997**, *283*, 1552–1562.

(114) Taipalensuu, J.; Tornblom, H.; Lindberg, G.; Einarsson, C.; Sjoqvist, F.; Melhus, H.; Garberg, P.; Sjostrom, B.; Lundgren, B.; Artursson, P. Correlation of Gene Expression of Ten Drug Efflux Proteins of the ATP-Binding Cassette Transporter Family in Normal Human Jejunum and in Human Intestinal Epithelial Caco-2 Cell Monolayers. *J. Pharmacol. Exp. Ther.* **2001**, *299*, 164–170.

(115) Mouly, S.; Paine, M. F. P-Glycoprotein Increases from Proximal to Distal Regions of Human Small Intestine. *Pharm. Res.* **2003**, *20*, 1595–1599.

(116) Mutch, D. M.; Anderle, P.; Fiaux, M.; Mansourian, R.; Vidal, K.; Wahli, W.; Williamson, G.; Roberts, M. A. Regional Variations in ABC Transporter Expression Along the Mouse Intestinal Tract. *Physiol. Genomics* **2004**, *17*, 11–20.

(117) Englund, G.; Rorsman, F.; Ronnblom, A.; Karlbom, U.; Lazorova, L.; Grasjo, J.; Kindmark, A.; Artursson, P. Regional Levels of Drug Transporters Along the Human Intestinal Tract: Co-Expression of ABC and SLC Transporters and Comparison with Caco-2 Cells. *Eur. J. Pharm. Sci.* **2006**, *29*, 269–277.

(118) Chen, X.; Chen, F.; Liu, S.; Glaeser, H.; Dawson, P. A.; Hofmann, A. F.; Kim, R. B.; Shneider, B. L.; Pang, K. S. Transactivation of Rat Apical Sodium-Dependent Bile Acid Transporter and Increased Bile Acid Transport by 1α,25-Dihydroxyvitamin D_3 Via the Vitamin D Receptor. *Mol. Pharmacol.* **2006**, *69*, 1913–1923.

(119) Meier, Y.; Eloranta, J. J.; Darimont, J.; Ismair, M. G.; Hiller, C.; Fried, M.; Kullak-Ublick, G. A.; Vavricka, S. R. Regional Distribution of Solute Carrier mRNA Expression Along the Human Intestinal Tract. *Drug Metab. Dispos.* **2007**, *35*, 590–594.

(120) Mitschke, D.; Reichel, A.; Fricker, G.; Moenning, U. Characterization of Cytochrome P450 Protein Expression Along the Entire Length of the Intestine of Male and Female Rats. *Drug Metab. Dispos.* **2008**, *36*, 1039–1045.

(121) Chow, E. C.; Maeng, H. J.; Liu, S.; Khan, A. A.; Groothuis, G. M.; Pang, K. S. 1α,25-Dihydroxyvitamin D_3 Triggered Vitamin D Receptor and Farnesoid X Receptor-Like Effects in Rat Intestine and Liver in Vivo. *Biopharm. Drug Dispos.* **2009**, *30*, 457–475.

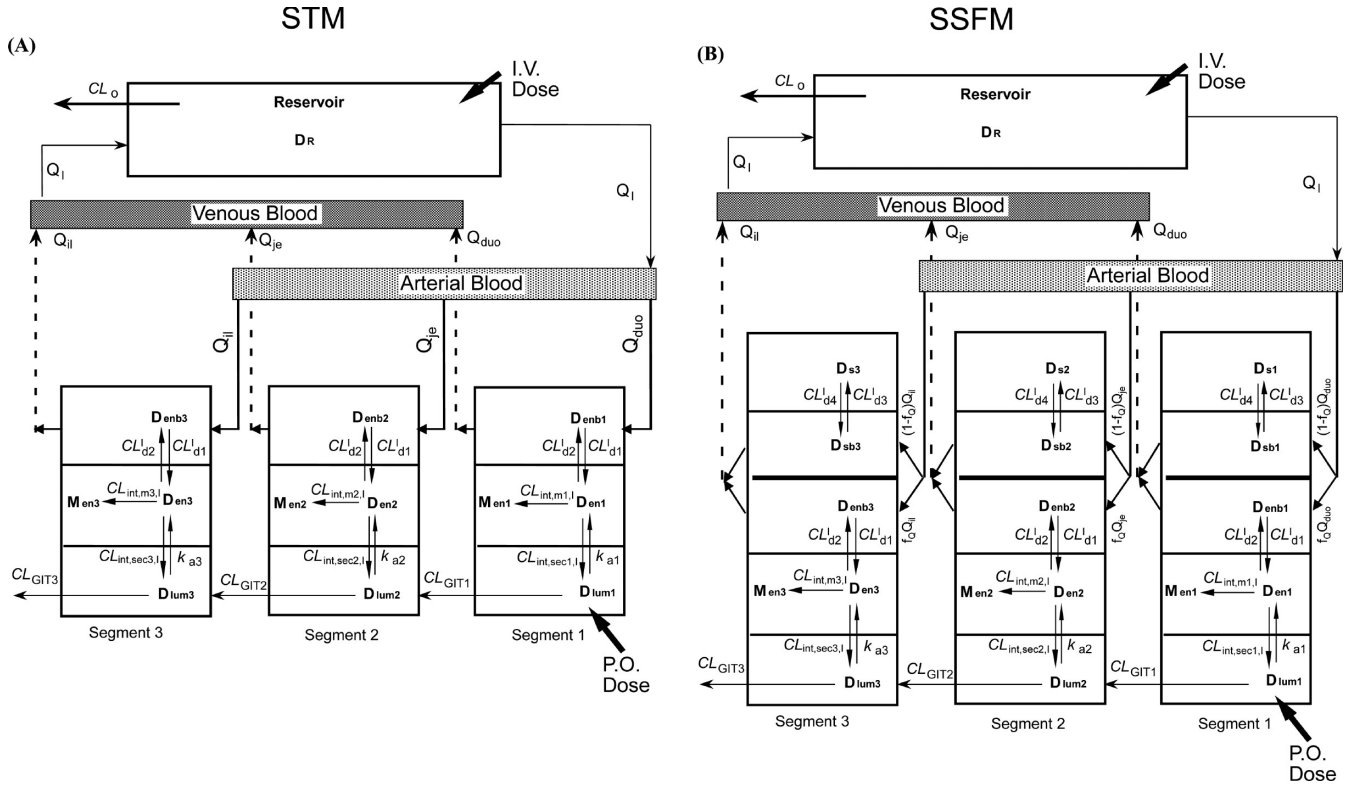

Figure 9. Schematic presentation of the segmental traditional model (STM) (A), and the segmental, segregated flow model (SSFM) (B) for intestinal absorption, metabolism, and secretion of substrates given orally or intravenously; the conditions considered mimic the recirculating perfused small intestine preparation with additional (parallel) clearances (CL_O) occurring within the central or reservoir compartment. (Reprinted with permission from ref 112. Copyright 2003 The American Society for Pharmacology and Experimental Therapeutics.)

weight of segment/weight of total segment) perfuses the entire segment, whereas in turn, only a portion (about 10%) of the segmental flow perfuses the enterocyte region of each segment of the SSFM.[2,112] The distribution of P450 that concentrates more in the proximal segment was found to be most important for drug bioavailability (Figure 10).[31,112,122] Yu utilized a seven segment advanced ACAT model that is similar to the STM which incorporated the distribution of CYP3A4 and P-gp along the human small intestine. The model further considers the dissolution, gastrointestinal transit and drug permeability. The resulting simulations predicted reduction of bioavailability due to P-gp-mediated efflux and metabolism of the parent drug. Upon usage of the ACAT model, Badhan et al. showed that increased metabolism ensued with increased secretion. The simulation of Badhan et al.[122] arrived at conclusions similar to those obtained for the Caco-2 system (Figure 4, middle panel) that increased secretion evoked increased metabolism. But, according to the equations chosen, saturable metabolism was indeed the case here.[122] Moreover, segregated flow to the enterocyte has not been considered in this simulation. Again, increased P-gp activity for drug efflux would not always bring about

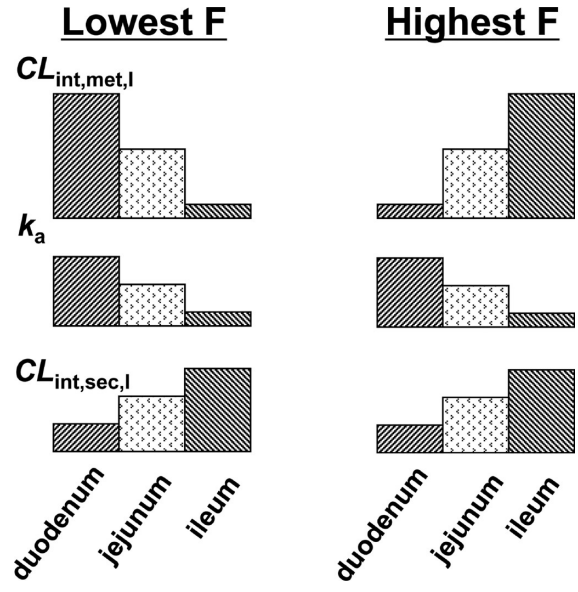

Figure 10. Segmental distributions of enzymes, apical absorptive transporters, and apical excretory transporters in segments of duodenum, jejunum and ileum, designated as $CL_{int,met,I}$, k_a and $CL_{int,sec,I}$. The distributions that showed the lowest *F* and highest *F* were shown (see ref 112 for conditions of simulations). (Reprinted with permission from ref 112. Copyright 2003 The American Society for Pharmacology and Experimental Therapeutics.)

(122) Badhan, R.; Penny, J.; Galetin, A.; Houston, J. B. Methodology for Development of a Physiological Model Incorporating Cyp3A and P-Glycoprotein for the Prediction of Intestinal Drug Absorption. *J. Pharm. Sci.* **2009**, *98*, 2180–2197.

increased MRT for the intact intestine, since the value of k_g in relation to k_a becomes important, as mentioned earlier (Tseng and Pang, unpublished simulations). Any proximally absorbed drug that reaches the systemic circulation would not be returned to the enterocyte region for secretion or metabolism readily according to the SFM and SSFM. Based on varying distributions of the metabolic intrinsic clearance ($CL_{int,met,I}$), the absorptive rate constants (k_a), and the secretory activity ($CL_{int,sec,I}$), the bioavailability of orally administered drugs (F) may be simulated. Indeed, according to both the STM and SSFM, the proximal distribution of CYP3A enzyme is the most important determinant conferring a low oral bioavailability (F), while the distributions of k_a and P-gp are less important (Figure 10).[112] Future models must thus consider the segmental, segregated flow model to render a greater prediction of drug oral bioavailability.

Examples. Data exists on saquinavir pertaining to single-pass intestine perfusion and *in vivo* in portal vein-cannulated rats under specific P-gp inhibition to elucidate the competition between transport and metabolism.[123] When perfused alone, saquinavir absorption in the jejunal region was very low. However, in the presence of the P-gp inhibitor, GF120918, the plasma concentration was increased by 24-fold while the amount of metabolite formed was increased by 20-fold. After oral administration of saquinavir to rats *in vivo*, the apparent oral clearance (CL/F) of saquinavir in GF120918-treated groups was decreased significantly, whereas the $AUC_{0-t}\{mi,P\}$ for the metabolites was increased, suggesting that the metabolic clearance of saquinavir was increased. These experimental data conform to predictions made from our PBPK intestine model (SFM and SSFM). K77, the dual CYP3A4 and P-gp substrate, was studied *in vivo* with the rat single-pass intestinal perfusion model.[124] Levels of K77 metabolites in perfusate and in blood in the presence of GF120918 were 1.5-fold higher than those of control, while the appearance of K77 in the mesenteric blood was increased 3-fold in the presence of GF120918.[122] These data again suggest that GF120918 is able to inhibit P-gp and increase K77 absorption across the intestine, allowing more drugs to enter the enterocytes for metabolism by the CYP3A4.

VII. Concluding Remarks

In this review, we utilized relevant catenary or PBPK models to describe the interplay between transporters and enzymes in Caco-2 cells or the liver and intestine, respectively. We included examples in the literature and commented on the expected interplay between transporters and enzymes based on the predictions from simulations with the solved equations against the experimental data. A reciprocal relationship between transporter and enzyme functionality or the seesaw (reciprocal) phenomenon for the interplay is the common observation. The scenario is altered with futile cycling or the interconversion between parent drug and metabolite, resulting in much greater complexity for the kinetics between the parent drug and the metabolite and their concentrations within cells. The concepts, based on PBPK models and the solved AUCs, should be useful tools to explain and expected changes in altered liver and intestine clearances in the presence of inhibitors or inducers of transporters and/or enzymes and in drug−drug interactions.

Acknowledgment. This work was supported by the Canadian Institutes for Health Research (MOP89850) and the National Research Foundation of Korea funded (NRF, 2009, 352, E0068).

MP900258Z

(123) Usansky, H. H.; Hu, P.; Sinko, P. J. Differential Roles of P-Glycoprotein, Multidrug Resistance-Associated Protein 2, and Cyp3A on Saquinavir Oral Absorption in Sprague-Dawley Rats. *Drug Metab. Dispos.* **2008**, *36*, 863–869.

(124) Cummins, C. L.; Salphati, L.; Reid, M. J.; Benet, L. Z. In Vivo Modulation of Intestinal Cyp3A Metabolism by P-Glycoprotein: Studies Using the Rat Single-Pass Intestinal Perfusion Model. *J. Pharmacol. Exp. Ther.* **2003**, *305*, 306–314.